University of South-Eastern Norway

www.usn.no

FMH606 Master's Thesis 2023

Engineering

Electrochemical systems of CO_2 reduction on carbon nanotube electrodes for biogas production using microbes as catalyst

Rahul Biswas

Candidate No: 8204

Faculty of Technology, Natural Sciences and Maritime Sciences

Campus Porsgrunn

University of South-Eastern Norway

www.usn.no

Course: FMH606 Master's Thesis, 2023

Title: Electrochemical systems of CO_2 reduction on carbon nanotube electrodes for biogas production using microbes as catalyst

Number of pages: 80

Keywords: Electrochemical reaction; CO_2 reduction; Methanation; Biogas upgrading; CH_4 production; Carbon nanotube electrode

Student: Rahul Biswas

Supervisor: Nabin Aryal, Md. Salatul Islam Mozumder, Vafa Ahmadi, Raghunandan Ummethala, Britt Margrethe Emilie Moldestad

External partner: University of South-Eastern Norway (USN), Porsgrunn

Summary:

This study explores electrochemical systems as an innovative approach for CO_2 utilization in biomethane production using the carbon-metal composite electrode material and microbes as catalyst. The emphasis has been given on developing biogas upgrading technologies, in response to the increasing demand for sustainable energy solutions. This thesis aims to investigate the electroreduction of CO_2 conversion into CH_4 on carbon nanotube-coated aluminium electrodes (Al/CNTs) with the assessment of current generation and methane production efficiency. The chronoamperometry method was applied to investigate the electrochemical reactions using methanogen mix-culture. The constant potential of -1.3 V vs. Ag/AgCl and gas composition was determined through gas chromatography (GC) analysis. The methodology also involved monitoring pH, alkalinity, volatile fatty acids (VFAs), and chemical oxygen demand (COD) variations over time. Also, scanning electron microscopy (SEM) imaging was employed to analyze the morphology of the electrodes. The Ex 2-Batch 3 experiment revealed a significant increase in biogas production achieving 3.66 mL/(cm^2 Al/CNTs surface area) over 20 days. At a current density of -0.488 mA/cm^2, the obtained CO_2 conversion efficiency, Faradic efficiency, and energy efficiency were 18.53%, 18.39%, and 3.12%, respectively. Finally, this research advances the concept of CO_2 reduction with Al/CNTs electrodes; however, challenges with electrode design, operation variables optimization, and insufficient long-term stability evaluations suggest areas that require further investigation and improvement in electrochemical CO_2 conversion for sustainable biogas upgrading.

Preface

This thesis was performed as part of the NORPART project #2021/10175 for the master's level full-time exchange program in Engineering, Autumn, 2023 at the University of South-Eastern Norway (USN), Porsgrunn.

The purpose of this research is to explore the electrochemical reduction of CO_2 conversion into CH_4 by using carbon nanotube-coated aluminum electrodes (Al/CNTs) which highlight the biogas production using microbes as catalysts.

I am extremely pleased to express my best regards, profound gratitude, deep appreciation, and heartfelt regards to my honorable supervisor Dr. Nabin Aryal, Associate Professor, Department of Process, Energy and Environmental Technology, USN, Porsgrunn, Norway, Dr. Md. Salatul Islam Mozumder, Professor, Department of Chemical Engineering and Polymer Science, Shahjalal University of Science and Technology, Sylhet 3114, Bangladesh, Vafa Ahmadi, Ph.D. Research Fellow, USN, Porsgrunn, Norway, Raghunandan Ummethala, R&D Manager, Nanocaps, Vestfold, Norway, and Dr. Britt Margrethe Emilie Moldestad, Professor, Department of Process, Energy and Environmental Technology, USN, Porsgrunn, Norway for their supervision, expert guidance, valuable instructions, scholastic direction, support, patience, and continuous encouragement throughout the successful completion of this study.

I am happy to note that I got immense help and cooperation from my lab mates and other laboratory staff for their help.

Finally, I would like to express my deepest gratitude and love to my respected parents for their dedication and many years of endless support to date that provided the foundation for this work.

Porsgrunn, January 26, 2024

Rahul Biswas

Contents

Summary: ... 2
Preface ... 3
Contents ... 4
List of Figures and Tables ... 6
Nomenclature ... 7
1 Introduction ... 9
1.1 Background ... 9
1.2 Methodology, objectives, task description and scope ... 13
1.3 Thesis report structure ... 14
2 Literature review ... 15
2.1 Electrochemical strategy for biogas upgrading ... 15
2.2 Electrochemical CO_2 reduction for biomethane production ... 18
2.3 Electrochemical process and operation ... 20
2.3.1 Electro-methanogenesis reactor ... 21
2.3.2 Electrocatalyst for electron transfer ... 25
2.3.3 Carbon nanotube-based electrodes ... 27
2.3.4 Electrolytes ... 29
3 Materials and methods ... 32
3.1 Materials ... 32
3.2 Electrochemical system operation ... 33
3.2.1 Experiment 1 ... 35
3.2.1.1 Aqueous media preparation by CO_2 saturation process ... 35
3.2.1.2 Ex 1-Batch 1 ... 36
3.2.1.3 Ex 1-Batch 2 ... 36
3.2.2 Experiment 2 ... 37
3.2.2.1 Ex 2-Batch 1 ... 37
3.2.2.2 Ex 2-Batch 2 ... 37
3.2.2.3 Ex 2-Batch 3 ... 38
3.3 Chemical analysis ... 38
3.4 Production analysis ... 38

3.5 Electrodes Fabrication 39
3.5.1 Sputtered Sample 39
3.5.2 Dip-coat 40
3.5.3 Chemical vapor deposition (CVD) 40
4 Results and discussions 41
4.1 Control experiment (Experiment 1) 41
4.2 Biomethane production (Experiment 2) 43
4.2.1 Current generation 45
4.2.2 Production efficiency 46
4.2.3 pH variation 48
4.2.4 Alkalinity determination 49
4.2.5 COD evaluation 50
4.2.6 VFAs analysis 51
4.3 Electrodes characterization 55
4.4 Limitations 58
5 Conclusion 59
5.1 Summary 59
5.2 Recommendations 60
References 61
Appendices 74
Appendix A: Thesis task description signed copy. 74
Appendix B: The thermodynamic potentials calculation of CO_2 reduction half reactions. 75
Appendix C: CH_4 production composition through electrochemical CO_2 reduction. 77
Appendix D: Production efficiency parameter of electrochemical reaction experiment. 78
Appendix E: Chemical composition analysis during electrochemical CO_2 reduction. 79
Appendix F: VFAs analysis during electrochemical CO_2 reduction. 80

List of Figures and Tables

Figure 2.1 Schematic diagram of electrochemical biogas upgrading. 16
Figure 2.2 Numerous reactor layouts for purifying biogas using microbial electrochemical techniques [20]. (A) Single-chambered design; (B) Double chamber set up; (C) Arranged in a triple chamber arrangement with anode, cathode, and regenerative unit; (D) Arranged in a four-chamber configuration with anode, regeneration, absorption, and cathode compartment; IEM- Ion exchange membrane. 22
Figure 2.3 Mechanism of electron transfer process from cathode for CH_4 production in electrochemical CO_2 reduction reaction. 27
Figure 3.1 Usages of the equipment for the experiment. (a) Thermo Scientific TRACE 1300 Series Gas Chromatograph; (b) GC- SRI 8610C, Multi-Gas#3 EPC configuration; (c) Potentiostat/Galvanostat/ZRA (Interface 1010 E, 29024, Gamry); (d) Centrifuge; (e) MT-00130 Spectroquant Spectrophotometer. 33
Figure 3.3 Electrochemical control experimental setup for CO_2 reduction to CH_4. 34
Figure 3.4 Electrochemical reaction (control experiment) running by applying voltage. 35
Figure 3.5 CO_2 saturation process experiment for making aqueous solution. 36
Figure 3.6 Electrochemical reaction running by applying voltage using Potentiostat. 37
Figure 3.7 Developed Al/CNTs working electrodes for electrochemical CO_2 reduction. 39
Figure 4.1 Current density of the electrochemical control experiment. 43
Figure 4.2 CH_4 generation from CO_2 electroreduction. 44
Figure 4.3 Broken electrodes during electrochemical operation. 45
Figure 4.4 Current density profile of CO_2 electroreduction into CH_4 generation. 46
Figure 4.5 CH_4 production efficiency from CO_2 conversion. 47
Figure 4.6 pH variation during electroreduction over time. 48
Figure 4.7 Alkalinity ($CaCO_3$) in a different time interval during CO_2 electroreduction into CH_4. 49
Figure 4.8 Total COD variation during methanogenesis. 51
Figure 4.9 Soluble COD variation during methanogenesis. 51
Figure 4.10 Butyric acid concentration during methanogenic microbial activities. 53
Figure 4.11 Propionic acid concentration during methanogenic microbial activities. 53
Figure 4.12 Acetic acid concentration during methanogenic microbial activities. 53
Figure 4.13 Isovaleric acid concentration during methanogenic microbial activities. 54
Figure 4.14 Isobutyric acid concentration during methanogenic microbial activities. 54
Figure 4.15 Isocaproic and heptanoic acid concentration in Ex 2-Batch 2. 54
Figure 4.16 SEM image of 200 nm Al/CNTs electrode. 56
Figure 4.17 SEM image of 250 nm Al/CNTs electrode. 57
Figure 4.18 SEM image of 300 nm Al/CNTs electrode. 57
Figure 4.19 SEM image of Al/CNTs electrode. 58
Table A.1 Amount of CH_4 production through CO_2 conversion. 77
Table A.2 CH_4 production efficiency parameter of electrochemical experiment. 78
Table A.3 pH, alkalinity, total-COD, and soluble-COD content during electrochemical reaction. 79
Table A.4 VFAs concentration during electrochemical CO_2 reduction. 80

Nomenclature

Abbreviations/Expressions	Description
Al/CNTs	Carbon Nanotube-Coated Aluminum Electrodes
CD	Current Density
CE	Counter electrode
CEM	Cation Exchange Membrane
CH_4	Methane
cm	Centimeter
cm^2	Square Centimeter
CNTs	Carbon Nanotubes
CO	Carbon Monoxide
CO_2	Carbon-Dioxide
CO_3^{2-}	Carbonate
COD	Chemical Oxygen Demand
Cu	Copper
CVD	Chemical Vapor Deposition
ºC	Degree Celcius
DEMS	Differential Electrochemical Mass Spectrometry
EE	Energy Efficiency
Eq.	Equation
Ex 1-Batch 1	Electrochemical Experiment First Batch
Ex 1-Batch 2	Electrochemical Experiment Second Batch
Ex 2-Batch 1	Bio-Electrochemical Experiment First Batch
Ex 2-Batch 2	Bio-Electrochemical Experiment Second Batch
Ex 2-Batch 3	Bio-Electrochemical Experiment Third Batch
F	Faradic Constant
FE	Faradic Efficiency
Fe	Iron
g	Gram
GC	Gas Chromatography
h	Hours
H_2	Hydrogen

H^+	Proton or Hydronium Ion
HCO_3^-	Bicarbonate
HER	Hydrogen Evolution Reaction
H_2S	Hydrogen Sulfide
IEM	Ion Exchange Membrane
kg	Kilogram
$KHCO_3$	Potassium Bicarbonate
kWh	Kilowatt Hour
M	Molarity
mA/cm^2	Milliampere Per Square Centimeter
min	Minutes
N_2	Nitrogen
$NaHCO_3$	Sodium Bicarbonate
NH_3	Ammonia
NH_4^+	Ammonium Ion
Ni	Nickle
nm	Nanometer
O_2	Oxygen
OER	Oxygen Evolution Reaction
OH^-	Hydroxil Ion
Pt	Platinum
pH	Potential Hydrogen
R	Universal Gas Constant
RE	Reference Electrode
RHE	Reversible Hydrogen Electrode
SEM	Scanning Electron Microscopy
SOFC	Solid Oxide Fuel Cells
SHE	Standard Hydrogen Electrode
V	Voltage
VFAs	Volatile Fatty Acids
vs.	Versus
WE	Working Electrode
µm	Micrometer

1 Introduction

This chapter provides a brief overview of the background, objectives, methodology, and significance of the study, serving as an introduction to the thesis. It addresses the rationale for studying electrochemical systems for CO_2 reduction on carbon nanotube electrodes in the context of biogas upgrading which clarifies the task description and scope of this thesis.

1.1 Background

In the present era, the major concern is that global warming is gradually growing due tohe accumulation of CO_2 in the atmosphere [1], [2]. One of the major sources of climate change is the combustion of fossil fuels [3], [4]. However, fossil fuels are the primary energy sources used nowadays on Earth to produce power and heat [5], [6], which results in an increase in the atmospheric CO_2 concentration [7]. Further, it is thought that non-renewable fuels are limited resources that are running out [8], [9]. Therefore, developing a new carbon cycle that can address the energy demands appears difficult. However, due to the low production rate and process expenditure, abilities for an industrial approach to converting CO_2 to fuels has not yet been developed [10], but it offers an alternative way to produce clean, renewable, and sustainable energy.

Meanwhile, significant carbon reserves are formed and stored as solid organic waste because of anthropogenic activity. These wastes can be transformed into biogas, which reduces the demand for natural gas extraction. Biogas is a valuable by-product of anaerobic microbial metabolism that uses resources such as organic waste materials, agricultural residues, wastewater, and municipal waste [11]. Generally, these different metabolic pathways produce biogas that contain a variety

mixture of compounds, namely methane (CH_4), carbon dioxide (CO_2), hydrogen sulfide (H_2S), ammonia (NH_3), hydrogen (H_2), nitrogen (N_2), oxygen (O_2), carbon monoxide (CO), and siloxanes, etc. The notable biogas composition is CH_4, CO_2, H_2S, and siloxanes where CH_4 content of 66.1% along with 33.3% of the second major element CO_2 of total volume [12]. These notable components in biogas except methane must be removed or converted into methane before gas application which is called biogas upgrading [13]. Moreover, the high CO_2 level in biogas drastically decreases the heat value, diminishes its energy density, and restricts its use as a clean energy source, therefore, requires additional processing when employed as a source of upgraded biogas [12], [14]. Additionally, the increased emission of such kinds of impurities in biogas is also detrimental to human health and bipgas appliances such as burners, engines [15], [16]. Therefore, intense research is being done on sustainable carbon capture and utilization technologies because of the urgent need to mitigate the detrimental effects of anthropogenic CO_2 emissions on the climate of our planet. Before usage as a biofuel, methane and CO_2 should be separated using the biogas upgrading technique [17]. The biogas upgrading process delivers biomethane with a purity of natural gas (more than 97% of CH_4), while other gases are separated and mostly discharged into the atmosphere [17], [18]. As a result, higher CH_4 concentration in biogas is associated with lower investment costs, carbon neutrality, and energy savings for upgrading [17], [19].

For biogas upgrading, there are several strategies for CO_2 reduction conversion into biomethane such as physiochemical, thermochemical, biochemical, photochemical, and electrochemical reduction systems [20]. For instance, recent commercial applications of physiochemical biogas upgrading techniques are membrane separation, cryogenic separation, pressure swing absorption, chemical adsorption, and water scrubbing [18]. However, it has been demonstrated that some of

commercial upgrading technology such as water scrubbers, amine-based, membrane etc. lead to higher energy, and corrosion issues in upgrading plants, as well as drastically influencing CO_2 and CH_4 emissions into the atmosphere [16]. Alternatively, the electrochemical CO_2 to methane production process has been reported as corrosion resistant process with least or no methane emission while operation is energy efficient. The CO_2 content from biogas can be utilized as resources for CH_4 productionThe electrochemical CO_2 reduction systems can generate a few different products (e.g., CH_4, higher hydrocarbons, etc.) following the conditions (e.g., pressure and temperature) of the atmosphere [21].

The capability of electrochemical technology to convert CO_2 into valuable hydrocarbons selectively makes it a promising biogas upgrading approach [22]. The formation of products (e.g., biomethane, CO etc.) through the electrochemical CO_2 reduction process is significantly more efficient than in traditional physicochemical reactors. This is likely due to the indirect reaction between precursors and intermediates resulting from the redox process on the catalyst surface, which can be readily adjusted by applying potential [23]. Since electrochemical CO_2 reduction offers all the already specified benefits, it is certainly the most prominent technique of CO_2 conversion into biomethane that simple process design and directs control of surface-free energy [24]. Whipple & Kenis (2010) stated that electrolysis at ambient conditions in an aqueous solution leverages the electrical driving force resulting in water splits and CO_2 reduction. A potential difference or voltage can be applied between the anode (water-splitting chamber following **Eq. 1.1**) and the cathode (CO_2 reduction chamber following **Eq. 1.2, 1.3, 1.4 and 1.5**) to allow the protons generated at the anode to cross a proton-conducting membrane and arrive at the cathode surface [23]. Different types of reactions might occur depending on the catalyst utilized and the parameters of the process.

$$2H_2O \rightarrow 4H^+ + 4e^- + O_2 \quad (1.1)$$

$$CO_2 + H^+ + e^- \rightarrow HCOO^- \quad (1.2)$$

$$HCOO^- + 7H^+ + 7e^- \rightarrow CH_4 + 2H_2O \quad (1.3)$$

$$CO_2 + 8H^+ + 8e^- \rightarrow CH_4 + 2H_2O \quad (1.4)$$

$$2H^+ + 2e^- \rightarrow H_2 \quad (1.5)$$

Moreover, it is reasonable to assume that the electrochemical cell configuration (e.g., solution flow agitation, electrode geometry) may impact the dynamics of the electrocatalytic CO_2 reduction reaction. Because the CO_2 concentration and interfacial pH can be directly affected by the hydrodynamics at the interface of the electrode and electrolyte [26], [27]. Besides, a batch-type cell is the most often used cell design, where the reduction process (**Eq. 1.4**) takes place at the cathode of an electrolyte that has been saturated with CO_2 (**Eq. 1.2**) [28], [29], [30]. Furthermore, in the context of electrochemical cell design and configuration, ideal conductive electrode materials should offer inherent benefits in anaerobic digester. For instance, adequate electrical conductivity, high surface area, recyclability, chemical stability, and biocompatibility should offer intrinsic advantages in the reactor to promote increased CH_4 production [31]. Dang et al. (2017) revealed that using carbon-based materials including carbon cloth, multiwall or single-wall carbon nanotubes, activated carbon, granular carbon, graphene, and graphite increases the formation of CH_4 [32]. Although carbon-based materials are frequently inexpensive, some of the carbonous materials have evolved into inactive materials, and their ability to transport electrons is merely possible in anaerobic digesters [31]. Additionally, the application of carbon-based materials was frequently restricted in terms of stability, reusability, conductivity, and surface area; hence, fabricating and implementing of spatial surface-modified materials was suggested. Aryal et al.

(2023) employed a carbon nanotube over conductive activated carbon bound with Fe nanoparticles which boosted CH_4 formation through direct intraspecific electron transfer [33]. Therefore, carbon nanotubes are a particularly intriguing category of carbon materials due to their distinctive structural and electrochemical characteristics. Consequently, carbon nanotubes offer a promising foundation for enhancing the catalytic activity of CO_2 reduction procedures, which could contribute to increased conversion efficiency and product selectivity. It has been reported the metal carbon composite electrode materials enhanced the CO_2 reduction capacity in electrochemical system when microbes are used as catalysts. Composite material such as carbon-metal, polymer-metal, polymer- carbon etc have been tested for the electrochemical CO_2 reduction process [31], [34].

1.2 Methodology, objectives, task description and scope

The focus and aim of this thesis work are to investigate electrochemical systems for CO_2 reduction in the generation of biomethane using microbes as catalysts called bioelectrochemical system with an emphasis on biogas production. A novel study into the application of Al/CNTs electrodes for CO_2 electroreduction is addressed in this thesis. A significant aspect of this study is that these specific Al/CNTs were fabricated by utilizing the laboratory of Nanocaps at Vestfold. The electrochemical cell using the Al/CNTs as cathode was used using microbes as catalysts.

The performance of the electrode was evaluated, and the reaction pathways were clarified by using chronoamperometry to investigate the CO_2 reduction reactions on the Al/CNTs with electron and current flow over time. CO_2 conversion into CH_4 was identified and quantified with the use of GC analysis. The effectiveness of CO_2 reduction in biogas streams for biomethane was also assessed using alkalinity evaluation, VFAs, total COD, and soluble COD measurement. This work gains a

unique perspective from its particular focus on evaluating the CO_2 reduction capabilities of Al/CNTs electrodes for biomethane formation in the context of biogas upgrading channels, as well as from the SEM analysis that explores their architectural features including structural morphology and surface characteristics. The complete task description (background and objectives) in detail is depicted in **Appendix A**.

1.3 Thesis report structure

The thesis report follows an organized framework with five chapters. Chapter 1 presents the introduction which provides an outline of the background, significance, and objectives of the research work of electrochemical system CO_2 reduction into CH_4 for biogas upgrading. Chapter 2 appears in the literature review, which provides a comprehensive review of the research findings relevant, to CO_2 electroreduction, operation modes and conditions using chronoamperometry procedure, several methanogenesis reactor design and production, electrocatalysts and their electron transfer mechanism, carbon-based nanotube electrodes, and electrolytes. Chapter 3 presents the materials and methods section which covers the experimental setup and operation design, procedures, chemical, and product analysis, as well as techniques employed in the research. Chapter 4 is offered in the results and discussions where outcomes from the experiments are presented and critically assessed in of the thesis findings. Finally, Chapter 5 summarizes the important results, consequences, limits, and potential future directions of the research, bringing the thesis report to a conclusion.

2 Literature review

The chapter on literature review provides a thorough investigation and analytical evaluation of relevant research about the electrochemical systems of CO_2 reduction on novel electrode impact and mechanism for upgrading biogas. This chapter attempts to recognize current research within the wider framework of scientific knowledge, offering a comprehensive overview of fundamental ideas, preceding approaches, and advances.

2.1 Electrochemical strategy for biogas upgrading

Electrochemical reaction is an effective technique that integrates electron flows with chemical changes in a reaction, frequently including electron or proton transfers. Chemical changes are frequently explained as the metal complex's oxide-redox reaction [35], referring to an electrochemical process that determines the correlation between a catalyst's activity and other properties and uses this information to improve the catalyst's selectivity and activity. Fundamentally, electrical energy is transformed into chemical energy and vice versa in the contact between an electrode and an electrolyte solution. Redox reactions, in which electrons pass between reactants and result in the formation of new chemical species, are important to electrochemistry. An electrochemical cell usually consists of electrodes submerged in an electrolyte solution, allowing current to flow through the cell. These cells can be organized based on their designs; **Figure 2.1** illustrates the electrochemical approach for biogas upgrading.

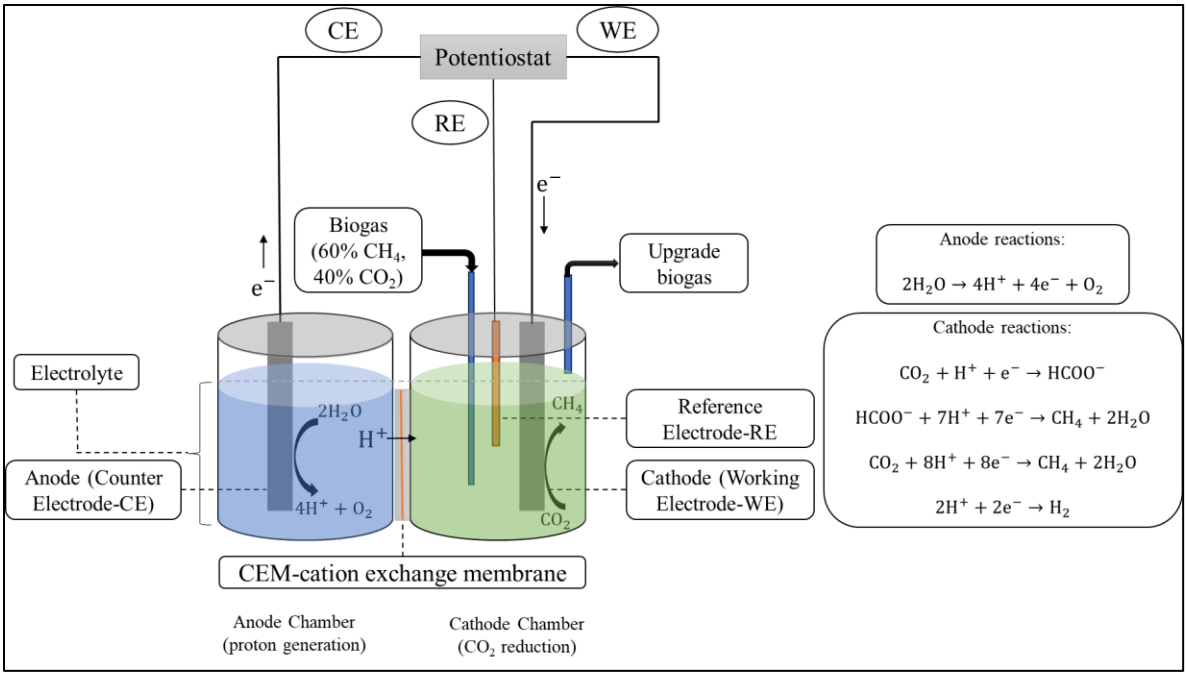

Figure 2.1 Schematic diagram of electrochemical biogas upgrading.

Electrochemical reactors possess substantial benefits over conventional heterogeneous chemical reactors. For example, their efficiency often surpasses that of chemical or combustion counterparts due to their independence from typical thermochemical cycles. Moreover, these reactors provide precise control of catalyst surface free energy through electrode potential, allowing for controlled reaction rates and route selectivity. In addition, complementary redox processes on distinct catalysts allow for the customization of properties necessary for each process individually, resulting in various reaction paths while avoiding rivalry between alternate routes. These distinct characteristics enable chemistry that are not possible in traditional systems. An et al. (1998) indicated hydrocarbon hydrogenation in an electrochemical reactor with a proton exchange membrane between the cathode and anode compartments [36]. This novel arrangement used water electrolysis at the anode to generate O_2 and H^+, which were then transferred to the cathode for H_2 reduction. The formed hydrogen gas interacted with diverse hydrocarbon attributes, demonstrating

significant advances. Through the elimination of potentially hazardous chemicals, the electrochemical method allowed for the high-selectivity emergence of the desired product, and it also reduced the energy and time requirements for synthesis [24]. These insights into these developments and their concrete benefits highlight the advantages and prospective use of electrochemical reactor advancements in various synthetic processes, such as biogas upgrading. The CO_2 fraction can be utilized from biogas for further methane production, thereby reducing the carbon footprint. Consequently, employing electrochemical methods for biogas upgrading involves utilizing such strategies to transform CO_2 into CH_4. The electrochemical cell, various catalysts can applied such as microbes, metals, polymers etc. [20] This method has the potential to improve biogas quality and energy content, allowing it to be used in natural gas systems or as a sustainable fuel source. However, the insufficient selectivity of the process is caused by the variety of feasible electrochemical pathways and their overlapping potentials. It is complicated to selectively convert the CO_2 from the gas mixer and to yield the desired, targeted product of choice. The reactivity of the CH_4 and the overlap of the potential ranges of CO_2 with other components of biogas are the primary causes of this poor selectivity [11]. Previous studies investigated several electrochemical setups, such as electrochemical cells, flow reactors, membrane reactors, and microbial electrolysis cells, to facilitate the conversion of biogas substances [20], [37], [38], [39], [40]. These investigations intended to optimize reaction conditions, improve selectivity, and increase overall efficiency in the electrochemical conversion of CO_2 and CH_4 into useful fuels. Electrochemical techniques for biogas upgrading encompass a wide range of procedures and inventions with the goals of increasing selectivity, optimizing conversion efficiency, and investigating new catalysts or electrode materials. These methods emphasize the significance of efficiency and selectivity in the upgrading, allowing regulated and unique transformations of

biogas components. Nevertheless, there are limitations in this process including issues with cost-effectiveness, the practicality of scaling up, electrode stability, and the requirement for additional improvements in energy efficiency and selectivity. Besides, the electrochemical conversion of biogas components may be highly selective and efficient, frequently requiring precise control over reaction conditions and electrode design. Therefore, in the field of biogas upgrading, overcoming these challenges is essential to the widespread application and commercial viability of electrochemical techniques.

2.2 Electrochemical CO_2 reduction for biomethane production

The use of electrochemical methods for CO_2 conversion and usage has recently gained appeal among researchers [25]. Chen et al. (2018) conducted an analysis that revealed that in 2017, the only expenses that would surpass the current market value of CO_2 would be the electricity used to convert it to CH_4 [41], however, the indirect value of upgrading the remaining CH_4 in the biogas to a useful product was not considered in this analysis. Moreover, various further techno-economic explorations have been conducted; the most recent study of Na et al. (2019) suggested that oxidizing organic compounds rather than water might result in even lower operational costs for CO_2 removal [42]. Research in this area intends to comprehend the mechanisms and reactions involved in this process. The basic idea of the operation is to drive the CO_2 reduction process at the cathode with an electric current, which produces CH_4. Daniels et al. (1987) first detailed the CO_2 reduction process of converting CO_2 into CH_4 in 1987, using elemental iron as the electron source for methanogens [43]. According to Cheng et al. (2009), the term "electro-methanogenesis" describes how electroactive methanogens promote CO_2 reduction through the formation of CH_4 by using electrons from the cathode or reducing equivalents [44]. For the electrochemical conversion of CO_2, a variety of methods have been studied at both high and low

temperatures, including gaseous, aqueous, and non-aqueous phase approaches. The reaction of electrochemical CO_2 reduction in aqueous conditions involves the transfer of multiple electrons and protons to reduce CO_2 into CH_4 [45]. The aqueous system, with its steady electrical conductivity and ease of concentration adjustment, is ideal for studying different electrode catalysts and their design features [46]. Through the reduction of the activation energy of the reaction and consequent increase in reaction rate, they speed up the conversion process. Reaction kinetics, product selectivity, and electrochemical process stability are all significantly impacted by the design and selection of catalysts. Electrochemical CO_2 reduction approaches include using various catalysts and electrolytes, adjusting operational factors such as current density, temperature, and pressure, and designing reactor setups to improve CO_2-to-CH_4 conversion efficiency.

Moreover, CO_2 conversions at high temperatures generally use solid oxide fuel cells (SOFCs), while low-temperature systems use transition metal electrodes in both aqueous and non-aqueous electrolytes including methanol, acetonitrile, propylene carbonate, or dimethyl sulfoxide [24]. Although a greater broad range of products is possible at low temperatures, SOFC devices frequently outperform low-temperature systems in terms of selectivity and performance [24]. Nevertheless, low-temperature electro-reductions, whether aqueous or non-aqueous, need several volts of applied potential, resulting in high power demands [24]. This addresses the systems and methods for electrochemical CO_2 reduction, emphasizing the products produced and evaluating their electrochemical performance and stability. Furukawa et al. (1999) used H_2 fuel to convert CO_2 into CH_4 and H_2O with yields of up to 80% utilizing a lower temperature (500 °C) SOFC cell with nickel/zeolite and silver electrodes [47]. Since most overpotentials are quite significant, H_2 often arises at the cathode not from the CO_2 reduction process directly but instead through the

concurrent hydrogen evolution reaction (HER) in either acidic or alkaline conditions [48]. Moreover, the complete electrochemical CO_2 reduction reaction in aqueous solutions involves multiple steps: CO_2 adsorption on catalyst surfaces, interactions among electrons, protons, and absorbed CO_2, and the subsequent release of synthesized valuable chemicals. The dominant reaction pathway, either CO_2 reduction or hydrogen evolution is contingent upon the stability of intermediates on active sites. When the *H intermediate is more stable on these sites, hydrogen evolution takes dominance; conversely, when $*CO_2$ is more stable than *H on catalyst surfaces, CO_2 reduction takes precedence [49]. CO_2 adsorption has a considerable impact on CO_2 reduction performance since it is a requirement for following reduction stages requiring electron transfer and causing a modification in the C═O bond shape from linear to bent, resulting in significant reorganizational energy expenditure [50]. However, CO_2 adsorption is impeded by the insufficient solubility of CO_2 in aqueous solutions such as 34×10^{-3} M at 25 °C [51], and the competitive nature of CO_2 reduction reaction and hydrogen evolution processes. Considering the two phases, the catalysts for the CO_2 to CH_4 conversion should concurrently maximize the binding strengths of *CHO and *CO [52]. Notably, the existence of the linear scaling relationship limits the possibility of the ideal binding strength of *CHO and *CO on a particular kind of active site [53]. However, an ideal catalyst should have a significant impact on a critical step or the important intermediates on its own [54]. Therefore, effective measures to modify or disrupt the linear scaling relationship should be implemented to achieve high catalytic activity and selectivity for the electrochemical conversion of CO_2 for biomethane production.

2.3 Electrochemical process and operation

Electrochemical processes include the conversion of chemical energy to electrical energy or vice versa at the contact between an electrode and an electrolyte solution. At this contact, oxidation and

reduction reactions occur, allowing the flow of electrons between the electrode and the chemical species in the solution. Fundamentally, these processes are controlled by the application of an external electric potential across the electrode-electrolyte interface, which drives the required electrochemical transformations. Electrochemical systems are generally comprised of three major components: electrodes, electrolytes, and an external electrical circuit. Electrodes operate as conducting surfaces on which electrochemical reactions occur, whereas electrolytes contain the ions required to support these processes. The external electrical connection permits electrons to travel between the electrodes, allowing the appropriate electrochemical reactions to take place. Electrochemical systems may selectively drive reactions such as CO_2 reduction by influencing parameters such as voltage, current, and reaction time, offering an adaptable framework for sustainable energy conversion and numerous industrial applications.

2.3.1 Electro-methanogenesis reactor

The design of the electrochemical cell, which influences the stability, Faradaic efficiency, and current density, is an important consideration in the CO_2 reduction process. For electrochemical CO_2 reduction systems in methanation, many cell designs have been employed and reactor vessels can be broadly categorized into H-type cells [55], polymer electrolyte membrane flow cells [56], microfluidic flow cells [57], solid oxide electrolysis cells [58], and DEMS cells [59]. Reactors are designed to offer reactions in a favorable environment, assuring high selectivity, efficiency, and stability throughout the process. Furthermore, the structures of reactor designs can be widely classified into different kinds, such as single-chamber, double-chamber, or multiple-chamber (e.g., three or four-compartment) configurations, each of which offers unique benefits and functionality as follows in **Figure 2.2**.

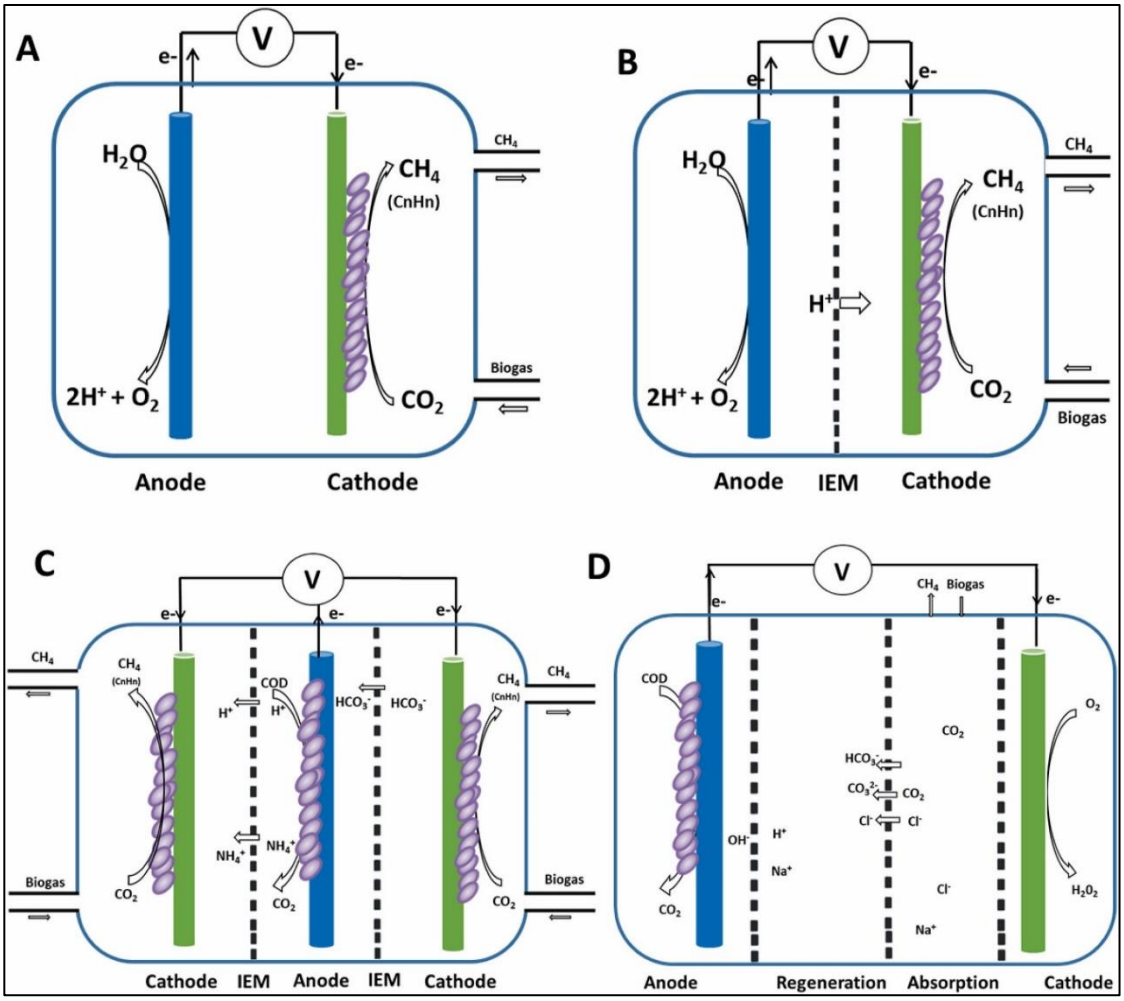

Figure 2.2 Numerous reactor layouts for purifying biogas using microbial electrochemical techniques [20]. (A) Single-chambered design; (B) Double chamber set up; (C) Arranged in a triple chamber arrangement with anode, cathode, and regenerative unit; (D) Arranged in a four-chamber configuration with anode, regeneration, absorption, and cathode compartment; IEM-Ion exchange membrane.

The single-chamber reactors frequently combine anodic oxidation and cathodic reduction within the same chamber without a membrane, allowing for direct interaction between the electrodes and biogas components and facilitating effective electrochemical processes [60]. Although it simplifies the setup, O_2 contamination in the single-chamber system can make it difficult to regulate reaction

kinetics and selectivity, which may hinder methanogen survival. The most well-known double chamber lab-scale reactor for the CO_2 reduction process that produces CH_4 is still the H-type cell, in which the counter electrode is placed in an anodic compartment and the working and reference electrodes are placed in a cathodic compartment [61]. Afterward, these two chambers are often coupled with a circular conduit and separated by an ion exchange membrane to prevent the reduced products from oxidizing once again during the process, exhibiting a characteristic 'H' arrangement. Nevertheless, both single-chamber and double-chamber reactors encountered issues such as the accumulation of volatile fatty acids (VFAs), notably acetate, which leads to greater toxicity owing to pH fluctuation. For instance, observations revealed an accumulation of VFAs including propionate and acetate, resulting in a pH drop from 7 to 6 in the single-chamber reactor [62]. This pH decline resulted in acidification, which adversely affected methanogen activity and hindered their function. Although partial alkalinity and buffering capacity serve to maintain pH levels, high concentrations can cause acidification, leading to a surrounding toxicity for methanogens [63], [64]. In addition, adding exogenous hydrogen to the reactor can encourage homo-acetogenic activity, which could allow acetate and other VFA to accumulate. The accumulation implies increased acetogenic and acidogenic activity, affecting the kinetic uncoupling between acid-forming and acid-consuming methanogens, which is essential for effective biogas formation [63]. Since there are no boundaries for ion movement in a single-chamber configuration, energy losses are reduced but unintended oxidation reactions at the anode may still occur. In contrast, a double-chamber reactor helps prevent undesired reactions by limiting conditions to the cathodic state, even if it may require a somewhat more energy demand.

Three-compartment reactors, which incorporate an accumulation chamber between anolyte and catholyte, effectively resolved issues concerning VFA accumulation and toxicity observed in single

and double-chamber configurations by facilitating the removal of excess VFAs and ions (e.g., NH_4^+ and HCO_3^-) from each side [65], [66]. In this configuration, the effectiveness was demonstrated by achieving over 90% CO_2 removal from biogas using 0.9 kWh electricity per kg CO_2, indicating higher efficacy compared to single or double chambers: with the three-chamber system effectively utilizing electrical energy for COD removal, CO_2 elimination, and ammonium bicarbonate recovery at the anode, cathode, and accumulation compartment, respectively [65]. Another study employed a three-compartment setup with a dual-sided cathode and a single anode compartment to remove and reduce CO_2 from biogas and performed greater reduction into CH_4 production, simultaneously promoting NH_4^+ transport from the anode to the cathode for nitrogen recovery from anaerobic digestion that demonstrated higher purity of ammonium recovery [67].

An enhancement in CH_4 production was attained by employing a microbial electrolytic capture, separation, and regeneration cell reactor with four membrane-separated compartments (e.g., cathode, absorption, regeneration, and anode) [68]. This configuration allowed it possible to treat household wastewater in the anode portion simultaneously with the removal or reduction of CO_2 at the cathode, thus, improving total energy efficiency. Moreover, multi-compartment reactor configurations, although more complex, have inherent benefits in electrochemical systems for biogas upgrading, including simultaneous treatment of wastewater at anode and upgrading of biogas, chemical production (e.g., VFA, acetate), reduced escape of CH_4 into the environment during upgrading, and CO_2, CO_3^{2-}, and HCO_3^- recovery at the regeneration and absorption compartment [65], [66], [67], [68]. Even though multi-compartment systems exceed single and double-compartment systems in terms of controlling pH and removing CO_2 [69], they have challenges scaling up because of issues with high energy consumption, low mass transfer rates, difficulties running continuously mode, and electrode fouling, which results in lower production

rates. Although tubular reactors for electrochemical-based biogas upgrading are still in the early phases of testing as viable alternatives.

2.3.2 Electrocatalyst for electron transfer

Several researchers have since published studies on different types of monocrystalline and polycrystalline metal electrodes for CO_2 conversion [70], [71], [72], [73]. Azuma et al. (1990) performed the electrochemical reduction of CO_2 at different temperatures by applying 32 metal electrodes, primarily transition metals, in $KHCO_3$ electrolytes [28]. Their investigations demonstrated that CH_4 production occurred, leading them to suggest a methodical rule for CO_2 electro-reduction on Cu metallic cathode electrodes. Because the group (Cu) can reduce CO_{ads}, relatively high current efficiencies of CH_4 can be achieved. Although Cu possesses an intermediate hydrogen overpotential, it is still possible to further reduce CO_{ads} to CH_4 because of its intermediate adsorption characteristic at room temperature. Moreover, Aryal et al. (2022) reviewed the several carbon-based electrodes that have been applied to assemble a three-dimensional structure for CO_2 reduction, including carbon felt, carbon paper, carbon brushes, carbon fiber, and reticulated vitreous carbon [20]. The three-dimensional structure of the electrode, notably exhibited by carbon felt which maximizes the active surface area, enabling efficient biofilm formation, electrode interaction, and electron transfer rates, is extensively studied in various electrochemical applications, especially, electro-methanogenesis, sensors, and microfluidic flow cells [74]. According to previous studies, graphite rod [22], plate, and carbon brush electrodes were investigated in biogas upgrading, observing that carbon brush electrodes produced approximately four times more CH_4 from CO_2 reduction than graphite plate cathodes [75]. This emphasizes the significant impact of electrode structure on CO_2 reduction, highlighting the function of catalytic active sites in supporting both direct and indirect electron transfer for CO_2 reduction, as illustrated

in **Figure 2.3**. A prior study investigated electro-methanogenesis, which produces CH_4 directly by absorbing electrons from the cathode surface [44]; another study explored CH_4 formation that happens during biogas upgrading, either directly by extracellular electron transfer or indirectly through H_2 mediation from the electrode [76]. The direct electron transfer mechanism for CO_2 reduction to CH_4 was observed in an enriched mixed culture dominated by Methanothrix and Azonexus species, implying that direct electron flow in electro-methanogenesis could provide higher efficiency by avoiding limitations related to redox reactions and mediator mass transfer [77]. The implantation of metallic electrodes, such as titanium woven wire mesh coated in platinum or stainless steel, resulted in high H_2 generation at the cathode and simultaneous biogas upgrading [78]. Metal-carbon composite electrodes of Cu-Ni and Fe coated onto graphite have also been used for biogas upgrading while investigating H_2 generation from metal cathodes; nevertheless, the electrode performance has obtained inadequate consideration [79]. The hydrogen evolution process (HER), which interacts with CO_2 reduction and is often more effective for most metals, must be considered when evaluating CO_2 reduction in aquatic settings. Remarkably, several catalysts used for CO_2 reduction were chosen because of their substantial overpotentials in HER rather than their ability to catalyze CO_2. Furthermore, extensive overpotentials also appear in HER for catalysts such as Sn, Pb, and Bi, which are often employed in electrochemical CO_2 reduction to formate [73].

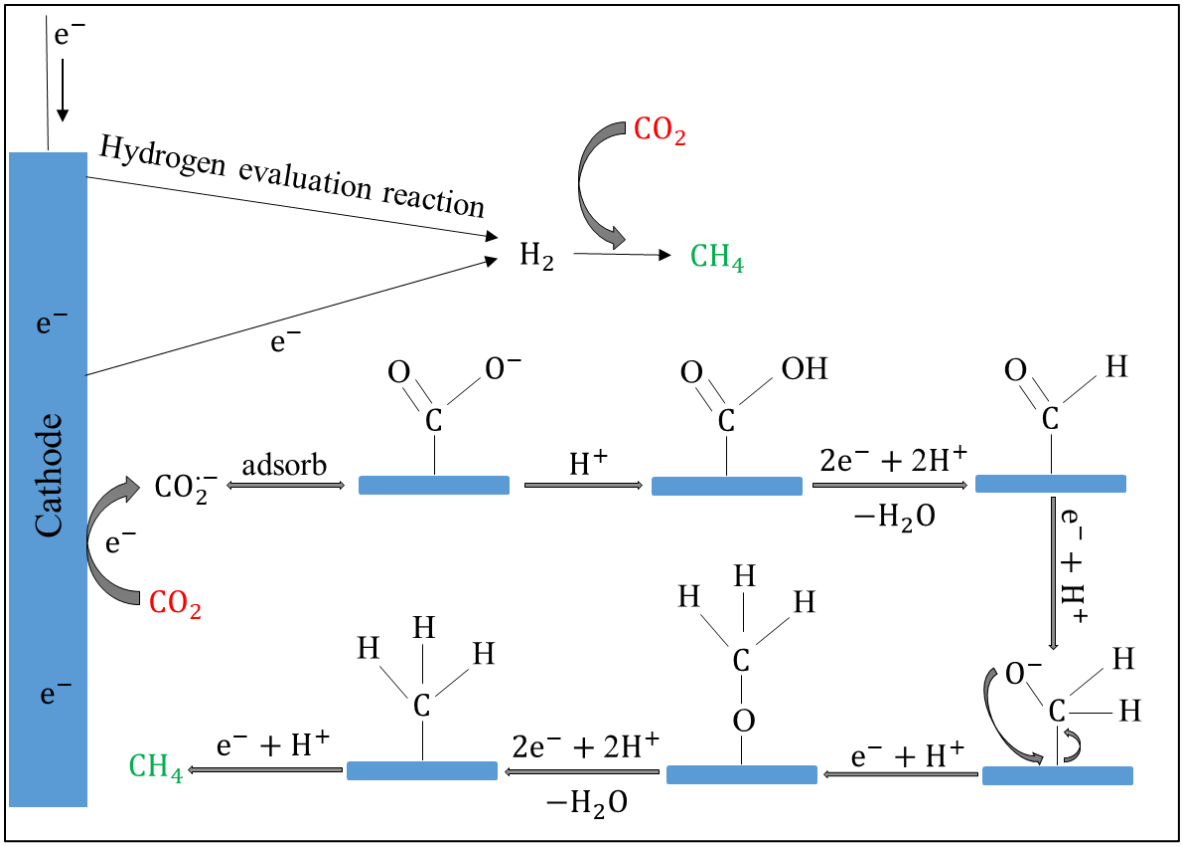

Figure 2.3 Mechanism of electron transfer process from cathode for CH_4 production in electrochemical CO_2 reduction reaction.

2.3.3 Carbon nanotube-based electrodes

In the recent advancement of electrochemical CO_2 reduction for CH_4 production, significant progress has been made, primarily focusing on the development of efficient electrocatalysts [80]. A significant way to fine-tune the electrocatalytic CO_2 reduction process is to modify the electrode size, shape, and crystallographic facets. For example, by modifying the limiting current density within particular potential windows, the shape of Cu catalysts might affect the selectivity of CO_2 reduction products [51]. It has been observed that the selectivity for CO_2 reduction products is influenced by the size of Cu nanocubes and octahedra; larger octahedral Cu nanocrystals are more favorable for overall CO_2 reduction and CH_4 production [81]. Furthermore, the

crystallographic facets of catalysts are important, as various facets display differential selectivity toward CO_2 reduction products (e.g., CH_4) [82], [83], [84]. Since twin boundaries on Cu electrodes demonstrated superior intrinsic CH_4 selectivity of 92% and high local current densities of 1294 mA/cm^2, defect engineering, including twin boundaries, has emerged as a promising method to improve the selectivity of CO_2 reduction towards CH_4 formation [85], [86]. In addition, A previous study revealed that the high density of edge sites from twin boundaries present in Cu nanowire catalysts results in better selectivity toward CH_4 production than other carbon products; nonetheless, authors found that the morphological alterations in the Cu nanowire had a significant impact on the selectivity toward CH_4. They resolved this dispute by using Cu nanowires/rGO wrapping to maintain the morphology of Cu nanowires, which allowed them to achieve 55% Faradaic efficiency toward at least -1.25 V vs. RHE using a fivefold twinned Cu nanowire [87]. The strain effects on adsorbate contacts and catalytic activity are demonstrated by Au-Cu core-shell nanoparticles, which exhibit adjustable catalytic performance based on the Cu layer thickness [88]. Cu-Ag alloys, although enhancing CO formation due to Ag possess a lower oxygen affinity, significantly increase CH_4 formation by moving *CO intermediates to Cu sites for subsequent hydrogenation [89]. This migration mechanism, which is dependent on Cu coverage inside the alloy, influences CO_2 reduction reaction selectivity [52]. Additionally, 1D structures such as Ag-modified Cu nanowires demonstrate increased CH_4 selectivity due to structural alterations that optimize CO_2 hydrogenation [90]. The significant CO binding of Pt and the strain effects of Cu provide difficulties for CO_2 reduction in Cu-Pt alloys. However, controlled Cu/Pt ratios in nanocrystals demonstrate potential in affecting selectivity towards CH_4 or H_2 evolution according to Cu and Pt atomic contents [91]. The efficiency and stability of catalysis may be improved by addressing the principles underlying catalyst degradation and by using support structures to

preserve nanostructures [92]. According to recent studies, using customized Cu nanocatalysts in GDE-based setups has boosted CO_2 reduction to CH_4 selectivity while minimizing H_2 evolution and improving product selectivity [81]. These novel catalyst designs and operational modifications have immense potential to enhance the efficiency and selectivity of electrochemical CO_2 reduction for biogas upgrading applications.

2.3.4 Electrolytes

Electrochemical CO_2 reduction is an intricate method that is considerably impacted by the type of electrolyte, which conducts the charge transfer between cathode and anode electrodes during chemical reactions [73], [93], [94], [95]. Even with the same metal electrode, various electrolytes might result in distinct product distributions [96]. Aqueous and nonaqueous electrolytes were among the several solutions from basic to acidic that were investigated as electrolytes [97], [98]. An aqueous electrolyte is produced by the dissolution of ions in a hydro-solvent. The primary benefit of this approach is its simple procedure and consistent electroconductivity, which allow control experiments with various catalysts [96]. This kind of electrolyte encourages HER, which often interacts with the CO_2 reduction process. Moreover, inadequate CO_2 solubility is another significant problem in an aqueous electrolyte [99], although numerous groups keep employing these. In the initial studies, frequently employed $KHCO_3$, which is the most widely used aqueous medium [71], [100], [101]. Traditionally, KOH has been employed as a CO_2 absorbent in industry to capture CO_2, which might be one cause. Eventually, the $CO_2/HCO_3^-/CO_3^{2-}$ equilibria lead the KOH to transform into $KHCO_3$ [102], [103]. Therefore, certain species such as HCO_3^- and CO_3^{2-} can be present in a $KHCO_3$ solution that has been saturated with CO_2, which would be favorable for CO_2 capture. However, the use of non-aqueous electrolytes has several benefits, such as enhanced CO_2 solubility in non-aqueous solutions and less complex analysis of the reaction

process by direct control over water content. For example, CH_3OH has five times the solubility of CO_2 as water and continues to serve as a CO_2 absorber in industry [104], [105].

Furthermore, it has been noted that the absence of water in non-aqueous solutions causes HER to be lower than in aqueous electrolytes, which is another reason why doing a CO_2 reduction experiment at low temperatures is favorable [73]. Besides, it has been found that greater activity is possible for some inert electrodes in aqueous solutions that become active in non-aqueous electrolytes [73], [93], [95], [96]. It should be mentioned that product separation and solvent recovery would cost more if volatile and toxic organic solvents were used [106]. Ionic liquid electrolytes, despite their infrequent usage owing to cost and sensitivity, represent an investigated alternative that typically enhances CO_2 reduction rates, presumably attributed to a reduced energy state of $*CO_2$ intermediates within the liquid-phase salt configuration, distinct from dissolved neutral molecules in solvents [107]. It is usually accepted that a comparatively substantial quantity of energy is required to transform a stable CO_2 molecule into $*CO_2$. When ionic liquids are present, complexation can occur by the interaction of CO_2 with the anion species (e.g., BF_4^- or PF_6^-) in the ionic liquid, leading to a reduction in activation energy [108]. The composition of the electrolyte, especially the cations and anions employed, has significant effects on the electrochemical conversion of CO_2, and solutions such as $KHCO_3$, Na_2SO_4, K_2SO_4, K_2CO_3, H_3PO_4, or $NaHCO_3$ provide suitable selections for this [109], [110], [111], [112]. Although the effects of cations or anions (e.g., HCO_3^-) on CO_2 electroreduction have not received much attention, it is frequently suggested that the type of electrolyte has a major role in selectivity and activity.

Additionally, maintaining a constant current on the Hg electrode, an increase in reduction potential initially was observed with increasing cation size (Li^+, Na^+, K^+, and Cs^+) [113]. Hori & Suzuki (1982) subsequently validated the phenomenon by revealing reduced overpotentials when

electrolyte concentration increased (e.g., Li^+, Na^+, and K^+) [114]. Another study reported a proportionate increase in the cathodic current peak magnitude on a Pd electrode with increasing cation size [115]. The variations in cation size affected CO_2 electro-reduction at Cu electrodes; larger cations raised production while reducing undesirable HER, with Cs^+ exhibiting the lowest reduction potential [116], [117], [118]. Due to cation adsorption and reaction kinetics at the outer Helmholtz plane, these observations underscore the influence that electrolyte cations have on the activity and selectivity of CO_2 electro-reduction. Notably, among the studied cations (Li^+, Na^+, K^+, and Cs^+) had the greatest hydration number and the most challenging adsorption onto the electrode, leading to greater HER due to decreased molecule stability on the electrode surface [73]. The previous study demonstrated the achievement of a high current density (-440 mA/cm^2) on an Ag electrode using a concentrated alkaline electrolyte (3 M KOH), attributed to increased K^+ concentration fostering a denser double layer at the electrode/electrolyte interface [119]. They also observed an increase in OH^- formation when using KOH as the electrolyte, leading to the usage of an anion exchange membrane to transport OH^- species to the anolyte, hence increasing CO_2 reduction by facilitating the oxygen evolution reaction (OER) [119]. The electrolyte concentration was shown to impact CO_2 reduction reaction products by modifying the pH at the electrode/electrolyte interface through variations in buffer capacity. The galvanostatic CO_2 reduction on Cu electrodes with varying $KHCO_3$ concentrations obtained the highest current efficiency from -5 mA/cm^2 current density at a significantly lower $KHCO_3$ concentration [120]. In another study, the potentiostatic techniques to investigate the impacts of $KHCO_3$ concentration on Cu cathodes, indicating the influence of both dissolved CO_2 and K^+ on product selectivity [121].

3 Materials and methods

This materials and methods chapter includes the experimental design and working procedure, materials used, reactor setup, methodologies, and operating parameters employed in conducting the research. This thesis work was performed in the Bio Lab, CO_2 Lab, and Kjemi Lab of Process, Energy and Environmental Technology, USN, Porsgrunn Campus. Further, SEM analysis characterization techniques were described for carbon nanotube electrodes. The Al/CNTs electrodes were collected from Nanocaps at Vestfold where they were fabricated, and their SEM experiments were analyzed in their laboratory.

3.1 Materials

In this study, a range of materials and equipment (**Figure 3.1**) was employed to facilitate the thesis experiment. A glass cylindrical vessel served as the primary containment unit for the reaction setups. The experimentation involved the utilization of specialized electrodes, including carbon nanotube-coated aluminum electrodes (Al/CNTs) and platinum electrodes. To control and monitor electrochemical reactions, a Potentiostat/Galvanostat/ZRA (Interface 1010 E, 29024, Gamry) was employed. Analytical instrumentation included gas chromatographs (GC- SRI 8610C, Multi-Gas#3 EPC configuration, Thermo Scientific TRACE 1300 Series Gas Chromatograph), a centrifuge, and an MT-00130 Spectroquant Spectrophotometer. Additionally, Spectroquant Test Kits/Cell for COD and alkalinity tests were utilized. Various chemicals and substances were essential for creating specific reaction environments and solutions, such as CO_2 gas, D (+) glucose, wastewater sludge inoculum, $KHCO_3$, $NaHCO_3$, yeast extracts, NH_4Cl, NaCl, $MgCl_2.6H_2O$, $CaCl_2.2H_2O$, formic acid, phosphate buffer solution, KCl, KH_2PO_4, and K_2HPO_4. These materials

collectively formed the essential components for conducting the experiments and analyses detailed in this thesis work.

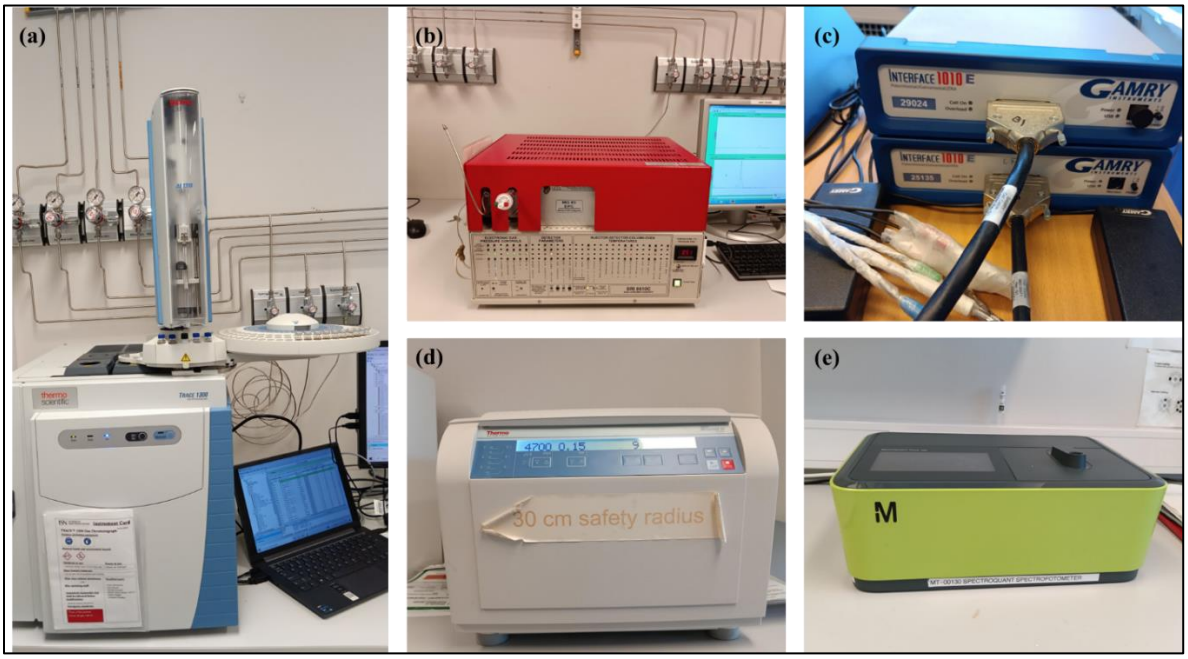

Figure 3.1 Usages of the equipment for the experiment. (a) Thermo Scientific TRACE 1300 Series Gas Chromatograph; (b) GC- SRI 8610C, Multi-Gas#3 EPC configuration; (c) Potentiostat/Galvanostat/ZRA (Interface 1010 E, 29024, Gamry); (d) Centrifuge; (e) MT-00130 Spectroquant Spectrophotometer.

3.2 Electrochemical system operation

Two 130 mL glass cylindrical-chamber electrolysis reactor chambers were separated by a cation exchange membrane (Nafion). In the anode chamber, 100 mL anolyte feed (1 M phosphate buffer, pH 7, conductivity 59.4 ms/cm) was used as the cation source 100 mL catholyte feed solution was used in the cathode chamber [122]. A carbon nanotube (Al/CNTs) was vertically inserted into the cathode in the chamber and platinum electrode was inserted in the anode chamber. Before the experiments, cathode chambers' headspace (30 mL) was flushed with pure CO_2 to remove the air

for maintaining anerobic condition. The headspace was filled with CO_2 with atmospheric pressure after the CO_2 flushing. The cathode chamber and one 100 mL gas syringe were connected to insert the CO_2 gas in the reactor and another syringe was connected to collect the producing gas sample for that converted from CO_2 by electrochemical reaction. A magnetic bar was moved at 200 rpm to agitate the electrolyte in both chambers. After that, the power supply was applied to a constant voltage of -1.3 V by using Potentiostat/Galvanostat/ZRA (Interface 1010 E, 29024, Gamry) equipment to perform direct electrolysis and the current flow was monitored through connecting laptop. The chronoamperometry electrochemical technique was used working, reference (Ag/AgCl), and counter electrode in the cell, where the counter electrode was inserted into the anode chamber. The experimental setup for the electrochemical operation is shown in **Figure 3.3**. After starting the reactor cell with a particular time interval, a gas sample was collected from the cathode chamber to determine gas composition by gas chromatography and was collected catholyte sample for chemical analysis as well. The equivalent catholyte was again filled by the initial feed and the anolyte was also replaced.

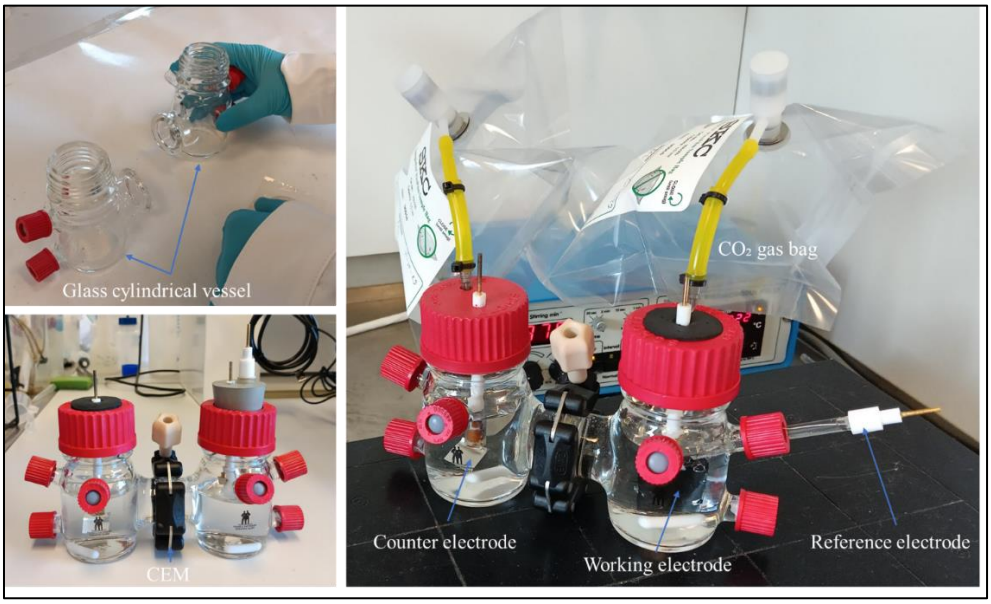

Figure 3.2 Electrochemical control experimental setup for CO_2 reduction to CH_4.

3.2.1 Experiment 1

In this experiment, the electrochemical reaction without catalyst was performed using saturated $KHCO_3$ and $NaHCO_3$ electrolytes as a control experiment for the conversion of CO_2 into CH_4 as shown in **Figure 3.4**. This is the control experiment without microbes.

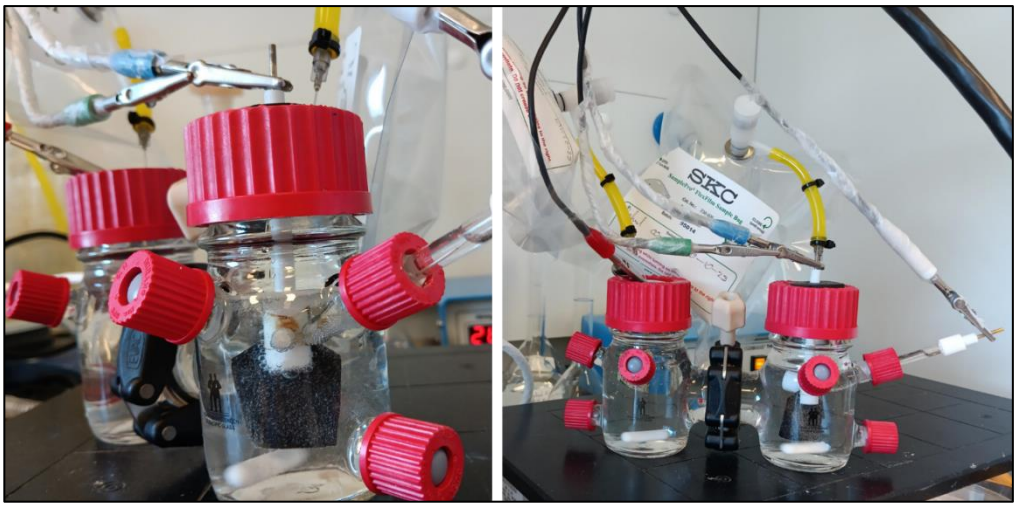

Figure 3.3 Electrochemical reaction (control experiment) running by applying voltage.

3.2.1.1 Aqueous media preparation by CO_2 saturation process

Using a gas dispersion device or a bubbler, 250 mL of separate solutions containing 0.5 M $KHCO_3$ or O.5 M $NaHCO_3$ were placed inside a round-bottom flask to introduce a controlled flow of CO_2 gas into the solution. To avoid moisture evaporation, distilled water containing a round-bottom flask was placed before the solution containing the flask. To ensure effective gas dissolution, gradually the CO_2 gas bubble was crossed through the solution while maintaining room temperature and atmospheric pressure. The overall experiment is shown in **Figure 3.5**. This process was continued until the solution achieved saturation, indicated by the point at which no further CO_2 dissolves in the solution which was observed by the weight gain of the solution through the measurement of the weight at specific intervals of time. The weight growth of the

solution is determined by measuring the weight at specific intervals of time, and this procedure is repeated until the solution approaches saturation, which is indicated by the point at which no more CO_2 dissolves in the solution. The procedure ended when the weight growth attained an equilibrium situation and the quantity of CO_2 that saturated the solution making it aqueous was calculated.

Figure 3.4 CO_2 saturation process experiment for making aqueous solution.

3.2.1.2 Ex 1-Batch 1

In the cathode chamber, 0.5 M $KHCO_3$ aqueous solution was used, and -1 V constant voltage was applied for 7 days. The working electrode dimension was 2.9 cm × 2.4 cm, and the area was 6.96 cm^2.

3.2.1.3 Ex 1-Batch 2

In the cathode chamber, 0.5 M $NaHCO_3$ aqueous solution was used, and -1 V constant voltage was applied for 7 days. The working electrode dimension was 3.2 cm × 2.6 cm, and the area was 8.32 cm^2.

3.2.2 Experiment 2

In this experiment, the electrochemical reaction was performed using a biocatalyst with phosphate buffer solution for the conversion of CO_2 into CH_4 as shown in **Figure 3.6**. The mix culture was used as biocatalyst.

Figure 3.5 Electrochemical reaction running by applying voltage using Potentiostat.

3.2.2.1 Ex 2-Batch 1

In the cathode chamber, 30% inoculum (inoculum contains 30% nutrients- 100 g/L NH_4Cl, 10 g/L NaCl, 10 g/L $MgCl_2.6H_2O$, and 5 g/L $CaCl_2.2H_2O$) and 70% 0.2 M phosphate buffer solution (pH 7) was used, and -1.3 V constant voltage was applied for 20 days [33]. The working electrode dimension was 3.2 cm × 1.6 cm, and the area was 5.12 cm^2. After 10 days, 20 mg/(100 mL inoculum) yeast extract was added to the cathode chamber.

3.2.2.2 Ex 2-Batch 2

In the cathode chamber, 30% inoculum (inoculum contains 20 mg/(100 mL inoculum) yeast extract, 20 mg/(100 mL inoculum) $KHCO_3$, and 30% nutrients- 100 g/L NH_4Cl, 10 g/L NaCl, 10 g/L $MgCl_2.6H_2O$, and 5 g/L $CaCl_2.2H_2O$) and 70% 0.2 M phosphate buffer solution (pH 7) was

used, and -1.3 V constant voltage was applied for 20 days [33]. The working electrode dimension was 4.0 cm × 2.7 cm, and the area was 10.80 cm^2.

3.2.2.3 Ex 2-Batch 3

In the cathode chamber, 30% inoculum (inoculum contains 20 mg/(100 mL inoculum) yeast extract, 20 mg/(100 mL inoculum) $KHCO_3$, and 30% nutrients- 100 g/L NH_4Cl, 10 g/L NaCl, 10 g/L $MgCl_2.6H_2O$, and 5 g/L $CaCl_2.2H_2O$) and 70% 0.2 M phosphate buffer solution (pH 7) was used, and -1.3 V constant voltage was applied for 20 days [33]. The working electrode dimension was 3.2 cm × 1.6 cm, and the area was 5.12 cm^2.

3.3 Chemical analysis

A benchtop multi-meter (HACH, HQ440d) was used to measure the pH and conductivity. The alkalinity ($CaCO_3$), total COD, and soluble COD were determined following Spectroquant Test Cell/Kits by using an MT-00130 Spectroquant Spectrophotometer equipment. The volatile fatty acids (VFAs) were determined by using Thermo Scientific TRACE 1300 Series Gas Chromatograph.

3.4 Production analysis

The gas composition was determined by using gas chromatography (GC- SRI 8610C, Multi-Gas#3 EPC configuration) and employing these data the CH_4 production and CO_2 consumption quantity was calculated. CO_2 conversion efficiency, Faradaic efficiency, energy efficiency, and current density were evaluated by using **Eq. 3.1, 3.2, 3.3, and 3.4**, respectively [123].

$$\mathrm{CO_2\ conversion\ efficiency\ (\%)} = \frac{\mathrm{CH_4\ production\ (mol)}}{\mathrm{CO_2\ quantity\ (mol)\ in\ headspace}} \times 100 \tag{3.1}$$

$$\mathrm{FE\ (\%)} = \frac{\mathrm{ZnF}}{\mathrm{q}} \times 100 \tag{3.2}$$

$$\text{EE}\ (\%) = \frac{E^{o} \times FE}{E^{o} + \eta + IR} \times 100 \tag{3.3}$$

$$\text{CD} = \frac{\text{total current (mA)}}{\text{unit area of the cathode (cm}^2\text{)}} \tag{3.4}$$

Where, FE = Faradic efficiency; CD = current density; EE = energy efficiency; Z = number of electrons exchanged for the product; n = the number of moles of the product; F = Faradaic constant (96485 C/mol); q = total charge applied (C); E^{o}= thermodynamic reaction voltage ($E^{o}_{cathode} - E^{o}_{anode}$) or the equilibrium cell potential for the desired product; η = sum of the overpotentials; and IR = ohmic loss across the cell.

3.5 Electrodes Fabrication

In the Nanocaps laboratory at Vestfold, the Al/CNTs electrodes were fabricated shown in **Figure 3.7** which was collected for my thesis experiment.

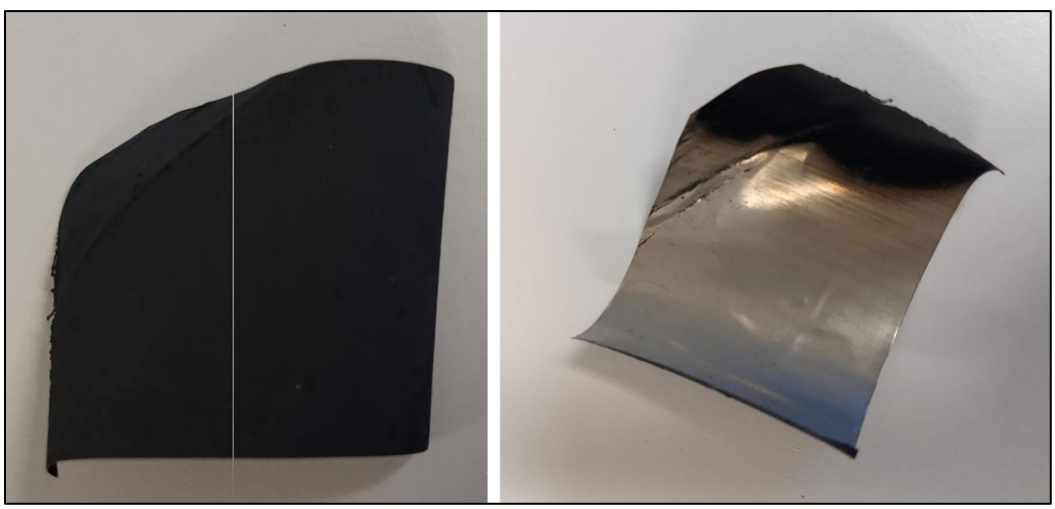

Figure 3.6 Developed Al/CNTs working electrodes for electrochemical CO_2 reduction.

3.5.1 Sputtered Sample

The samples that were sputtered with nickel were made with an AJA International DC magnetron sputtering facility, model ATC 20x20x30. The substrates were 70 µm pre-etched aluminum foils,

and the target was pure Ni (99.999%). To promote greater uniformity, the depositions were performed at a power of 25-300 W and a sample rotation speed of 10-20 turns/minute. According to the analysis of a planar reference crystal, Ni has a thickness of 200-300 nm.

3.5.2 Dip-coat

The selected substrates were immersed in the solution using a petri dish to start the dip coating process. To produce a uniform coating on both sides of the substrate, the immersion process was carried out four times, for five minutes each. The samples were dried on a hot plate to passively dry them after each dip coating to ensure the ethanol could evaporate. This intermediate drying phase was vital in rapidly settling the coating and facilitating uniform layer distribution over the underlying surface.

3.5.3 Chemical vapor deposition (CVD)

The experiments were intended to determine the effect of different factors, such as gas ratio, flow rates, and process time, on the yield and quality of carbon nanotubes (CNTs). The temperature was precisely regulated at 580 ºC to retain the structural integrity of the substrate, notably aluminum, which has a comparatively low melting point of 660 ºC. This guaranteed that the thin foil substrate remained intact throughout the CNTs manufacturing process. The selected gas ratio for CVD was determined using a gas ratio of 1:5:2 (Ar: H_2: C_2H_2), based on conditions set up in a reactor on a laboratory scale. With this modification, the parameters that achieve the maximum yield in the synthesis of CNTs were optimized. The CVD procedure spanned from 20 min to 3 h.

4 Results and discussions

In this results and discussions chapter, the production of CH_4 from CO_2 electroreduction is presented and described. CO_2 conversion efficiency, current density, Faradic efficiency, and energy efficiency result from the experiment data are determined and critically analyzed for their significance, elucidates patterns or correlations observed along with the SEM images data of Al/CNTs electrode, thereby providing a comprehensive understanding of the implications and contributions of the research in the context of electrochemical biogas production.

4.1 Control experiment (Experiment 1)

The electrochemical conversion of CO_2 into CH_4 was catalyzed by two distinct batches using saturated $KHCO_3$ and $NaHCO_3$ aqueous solutions in the experimental setup. Following the process of CO_2 saturation, the saturation values for $KHCO_3$ at 30 min and $NaHCO_3$ at 35 min were found to be 0.0016 g/mL and 0.00268 g/mL, respectively, signifying the achievement of CO_2 saturation in those solutions for making aqueous solution. However, the desired CH_4 generation did not materialize after the solutions were exposed to a continuous electrochemical reaction for 7 days at a constant voltage of -1 V. The current profile of these electrochemical experiments is shown in **Figure 4.1**. Furthermore, when $NaHCO_3$ was used, a negative event was observed as the working electrodes degraded and broke down, ultimately blending with the solution. This unexpected result raises important issues that need to be addressed. In contrast, the use of $KHCO_3$ was found to be less disruptive, emphasizing the potential impact of the carbonate source on the structural integrity of the aluminum-based electrodes.

Although the electrochemical procedure was applied, no methane was produced, which might indicate that the experimental conditions were insufficient or ineffective. The lack of intended methane generation might be attributed to factors such as electrode composition, surface shape, and reaction parameters. When $NaHCO_3$ is used, the breakdown and corrosion of working electrodes indicate potential electrode-material compatibility difficulties or an undesirable interaction between the electrolyte and electrode material. One of the possible causes of the electrode failure is the corrosive nature of the electrolyte, which may have caused the electrode material to degrade. The selection of $NaHCO_3$ may have caused harsher conditions, which resulted in the breakdown that was observed in the aluminum-based electrodes; perhaps, because of its increased ionic strength or pH variation, associated with the susceptibility of aluminium to corrosion in alkaline solutions. Because NaOH and KOH are known to corrode aluminum alloys, they were not regarded as inhibitors under the experimental conditions and the absence of NH_4OH, a known inhibitor, may have caused the corrosion [124]. Moreover, the structural integrity of the electrodes might have been damaged due to continuous exposure to high voltage, resulting in their disintegration.

Therefore, a biocatalyst inoculum was added to the electrochemical system in subsequent experiments to solve the problem of CH_4 generation. CNTs enhance CH_4 production in anaerobic processes by promoting direct interspecies electron transfer between bacteria and methanogens [125]. In methanogenic processes that are developed, conductive materials have the potential to increase the generation of CH_4. Biofilms that are engineered and release polyglutamate or polyaspartate are used to prevent corrosion on aluminium alloys. The mechanism involved in this biofilm-retained inhibitory species is more complex than just lowering the O_2 content at the metal surface [126]. Through employing the biocatalytic potential for CO_2 electroreduction, this phase

attempted to produce CH_4 through the biologically mediated process and increased catalytic activity. The use of a biocatalyst as an inoculum indicates a strategic shift in technique, utilizing biological pathways to facilitate CO_2 reduction and demonstrating the adaptability of the experimental approach.

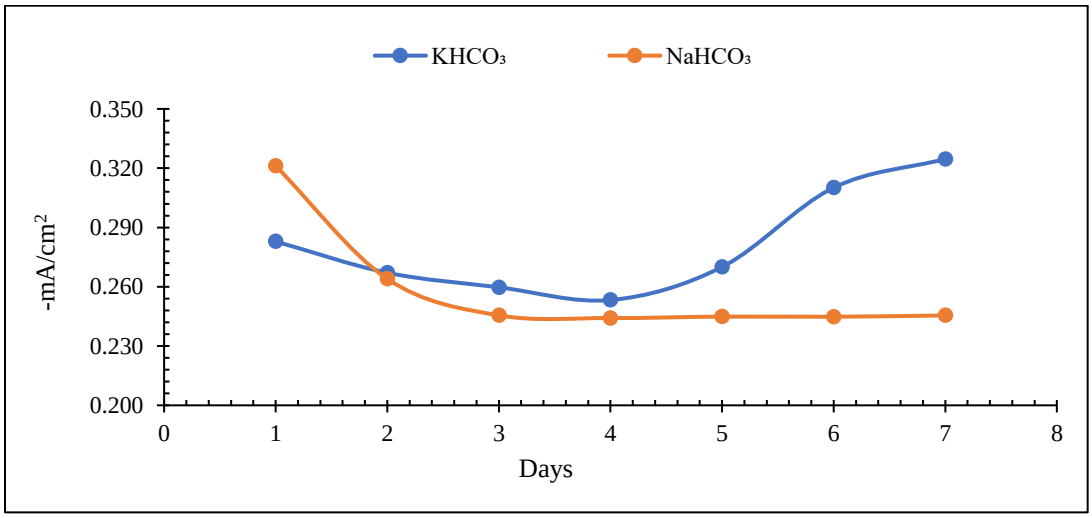

Figure 4.1 Current density of the electrochemical control experiment.

4.2 Biomethane production (Experiment 2)

The generation of CH_4 from CO_2 reduction per Al/CNTs electrode surface area is illustrated in **Figure 4.2** for different periods. In Ex 2-Batch 1, the highest CH_4 production of 4.08% was observed during the first 10 days of the experiment, which was conducted as a control using a biocatalyst. However, when a yeast mediator was used after the second 10 days, the maximum CH_4 production was demonstrated to be 22.84%. Ex 2-Batch 2 exhibited greater CO_2 reduction and CH_4 production with a shorter time interval, although after producing 18.97% CH_4, the working electrode broke down (**Figure 4.3**), resulting in zero production after 8 days. Besides, Ex 2-Batch 3 performed smoothly and CH_4 production was found in the range of 10.95-21.16%. A previous study employed a molten-salt-based electrolytic reactor with partitioned electrolysis

chambers for continuous CO_2 capture and reduction, resulting in a yield of 33.26% of CH_4 [127]. Since the batch process of CO_2 flow into the headspace of the reactor was applied, the CO_2 was not captured continuously in our experiment; nonetheless, the findings exhibited more comparable higher biomethane production. Furthermore, the addition of yeast extract to the electrochemical system may impact CH_4 generation through various mechanisms involving microbial stimulation, changes in substrate availability, pH or ionic composition changes, and interactions with electrochemical reactions. The addition of yeast extract is known to enhance CH_4 production in anaerobic digestion [128]. However, it is crucial to note that our study did not find CH_4 from anaerobic digestion, while bioelectrochemical processes showed an increase in CH_4 production with yeast extract. A control batch of syringes with yeast extract was run to distinguish the specific impact of yeast extract on bioelectrochemical CO_2 reduction; whereas yeast extract was an effective growth promoter of anaerobic microorganisms in electrochemical conversion [129].

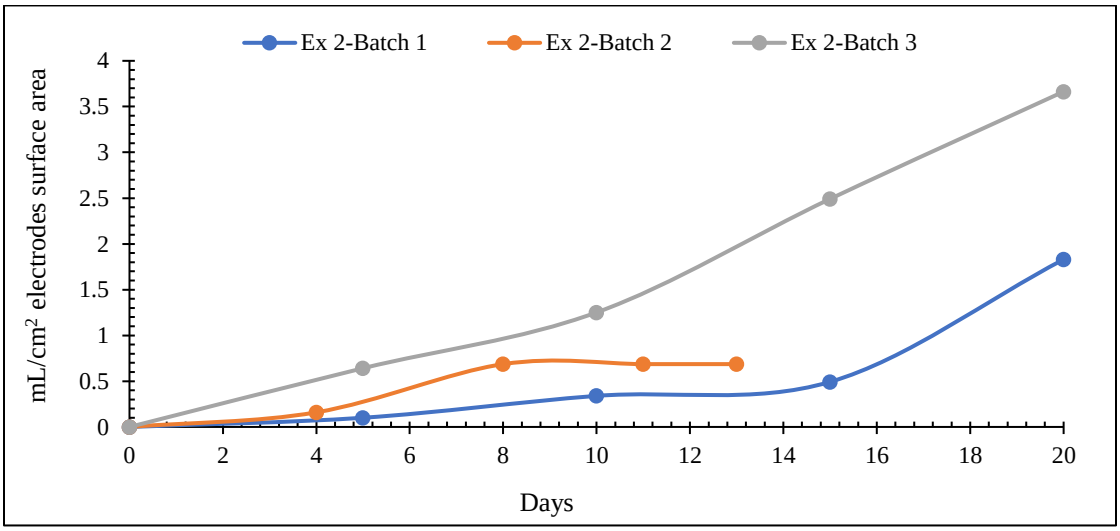

Figure 4.2 CH_4 generation from CO_2 electroreduction.

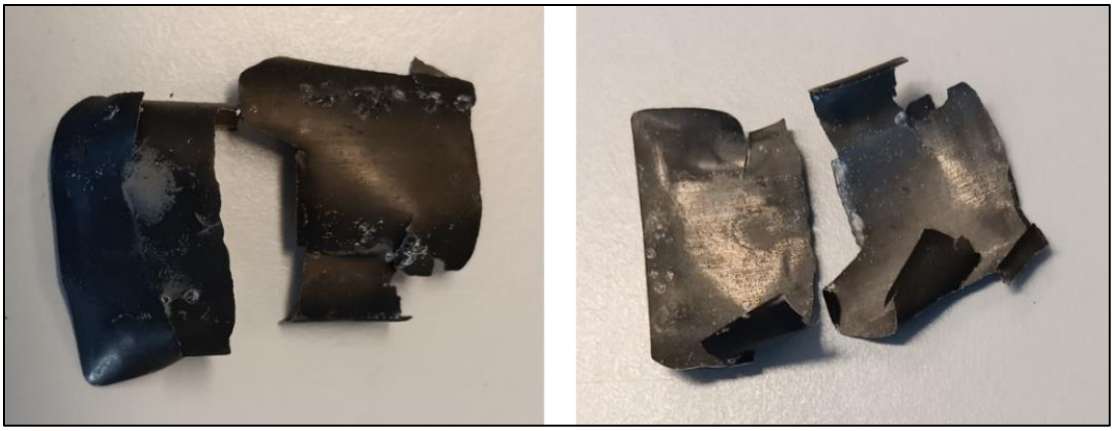

Figure 4.3 Broken electrodes during electrochemical operation.

4.2.1 Current generation

The experiment was carried out with a constant voltage of -1.3 V vs. Ag/AgCl (-1.1 vs. SHE), and the findings indicated distinctive patterns in current density for each batch (**Figure 4.4**) and higher surface area electrodes generated higher current which influenced the efficiency of CH_4 synthesis. The consistently increased current density in Ex 2-Batch 3 correlates with efficient CO_2 electroreduction, leading to steady and considerable CH_4 generation. The shifts in current density imply that dynamic electrochemical processes are involved in higher yields of CH_4. Moreover, Ex 2-Batch 2 exhibited effective CO_2 reduction and CH_4 generation in a shorter period, despite a lower declining trend in current density. The synthesis of CH_4 was interrupted by the early breakdown of the working electrode which emphasized the vital role that electrode stability plays in maintaining efficient electrochemical processes. The slightly decreasing trend in current density in Ex 2-Batch 1 did not affect CH_4 production. The addition of a yeast mediator greatly enhanced electrochemical efficiency, resulting in a remarkable increase in CH_4 generation. The previous research reported -0.36 and -1.6 mA/cm^2 current density on carbon paper electrodes and Cu complex-derived catalysts, with CH_4 generation of 355 ppm and 455.5 ppm, respectively [130]. The mixed culture electrochemical *in-situ* batch system on carbon brush electrodes reported a

lower current density of 0.407 mA/m^2 with an efficiency of 18.8% which indicates the analogous results with our findings. [75].

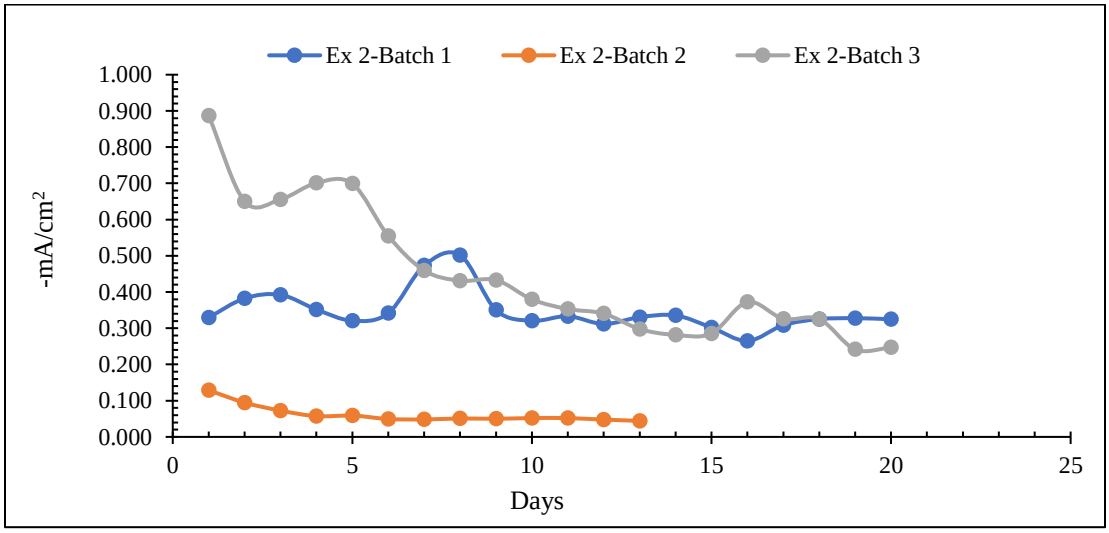

Figure 4.4 Current density profile of CO_2 electroreduction into CH_4 generation.

4.2.2 Production efficiency

The effectiveness and stability of CH_4 synthesis from CO_2 electrochemical conversion were evaluated through CO_2 conversion efficiency, Faradic efficiency, and energy efficiency, as illustrated in **Figure 4.5**. The efficiency of converting CO_2 into CH_4 is directly reflected in CO_2 conversion efficiency. A greater amount of CO_2 is effectively converted into CH_4 when the CO_2 conversion efficiency is higher and 0.94 mL/day CO_2 reduction rate, indicating a more stable and optimized electrochemical process which was revealed at higher current density in Ex 2-Batch 3; although at lower current density showed greater CO_2 conversion efficiency with a CO_2 reduction rate of 0.93 mL/day because of the mechanical disruption in Ex 2-Batch 2. Furthermore, Ex 2-Batch 1 exhibited the -0.346 mA/cm^2 average current density with 9.67% Faradic efficiency and 1.64% energy efficiency over the Al/CNTs cathode efficiency with a CO_2 reduction rate of 0.47 mL/day. In contrast, the lower average current density at -0.062 mA/cm^2 was found with higher

Faradic efficiency and energy efficiency of 31.26% and 5.30%, respectively in Ex 2-Batch 2. However, CO_2 reduction Faradic efficiency of 18.39% and energy efficiency of 3.12% were demonstrated at the higher average current density of -0.488 mA/cm^2 in Ex 2-Batch 3. Two primary reasons for the substantial increase in Faradaic efficiency can be observed in the Al/CNTs cathodes at higher current densities. First, when overpotentials rise, the kinetics of the readily facilitated HER accelerate more quickly than those of the slow CO_2 reduction reaction. Secondly, the limited mass transfer of CO_2 is impacted by the excess water present at the cathode [131]. Consequently, In our experiment, the overpotential was -0.86 V and the Nafion exchange membrane in the cathode catalyst layer facilitates the CO_2 mass transfer of the cathode. The *in-situ* biogas upgrading and microbial electrochemical CO_2 reduction study revealed an approximate 22.9% CO_2 conversion rate [132], whereas the bio-electrochemical conversion of CO_2 to CH_4 obtained 1.6 mL/day of CH_4 production at a lower current density of 0.04 mA/m^2 [133].

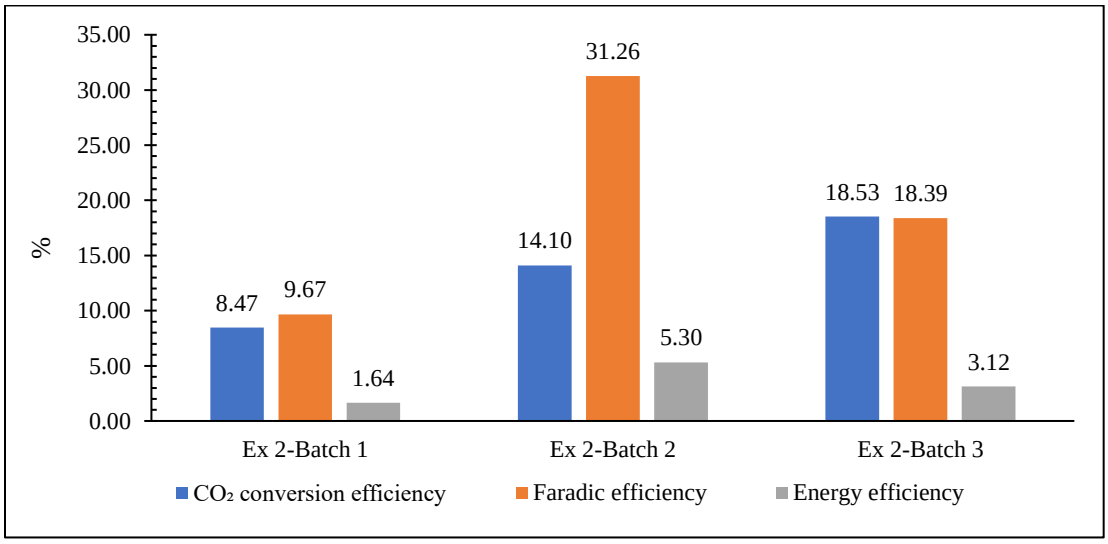

Figure 4.5 CH_4 production efficiency from CO_2 conversion.

4.2.3 pH variation

In electrochemical systems, pH is a key variable that influences the effectiveness of CO_2 capture efficiency and the conversion of CH_4 that is produced. The pH variations observed in experimental Batches 1, 2, and 3 are depicted in **Figure 4.6**. The pH in Ex 2-Batch 1 increased gradually from its starting value of 7 to a peak of 8.34 on day 5 before declining. Similar variations in pH over time were observed in Batches 2 and 3, although with distinct patterns. This dynamic variability points to a gradual shift in the basicity ($[OH^-]$) or acidity ($[H^+]$) of the solution. The exchange of ions occurs often during electrochemical processes, and this can affect the pH of the solution. The pH variations that have been observed may be explained by a variety of electrochemical events, the production of intermediates, the development of hydrogen, and changes in the concentration of buffer species. These findings indicate the complex interplay of simultaneous reactions that impact the chemical composition of the solution. In contrast to the other experimental sets, Ex 2-Batch 2 showed fewer noticeable pH changes, which might be the consequence of altered reaction pathways or decreased side reaction intensities. The observed reduction in CO_2 and increase in CH_4 might be associated with favorable reaction kinetics induced by pH changes, which improve CO_2 conversion to CH_4.

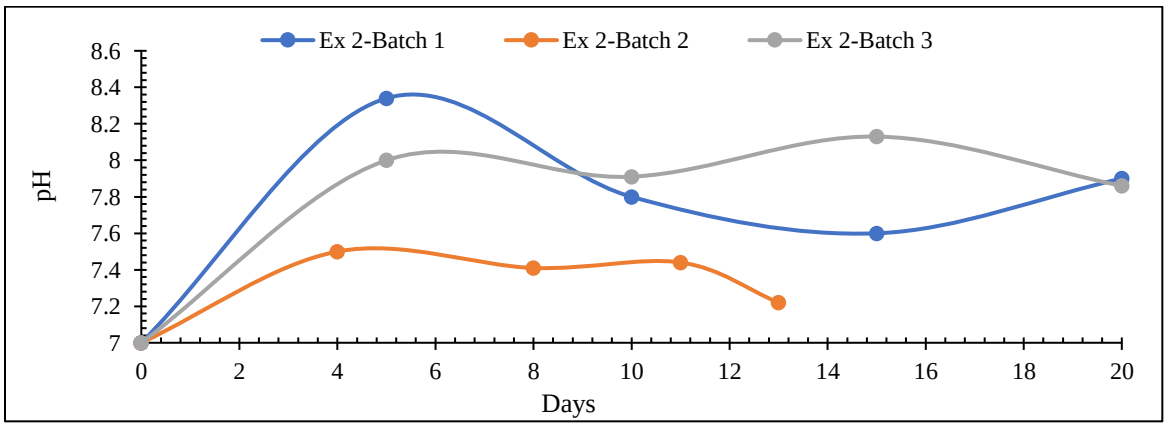

Figure 4.6 pH variation during electroreduction over time.

4.2.4 Alkalinity determination

Alkalinity was measured in terms of $CaCO_3$ for CO_2 electrochemical conversion into CH_4 throughout the period depicted in **Figure 4.7**; it indicates the alkalinity of the solution in terms of its corresponding concentration of calcium carbonate. An increase in alkalinity might indicate a stronger buffering capacity, indicating the capacity of water to resist changes in pH. This is due to dissolved CO_3^{2-}/HCO_3^-. However, the alkalinity increased after 4 days and drastically declined after 8 days in Ex 2-Batch 2, whereas CH_4 production was revealed at 5.75% and 18.97%, respectively. The drastically decreased alkalinity after 8 days indicates the CO_3^{2-}/HCO_3^- in the solution may react with H^+ and electrons and convert into CH_4. Nevertheless, the broken working electrodes could not transfer the electron into the solution and CO_3^{2-}/HCO_3^- did not convert into the CH_4 after the next observations. In Ex 2-Batch 3, alkalinity fluctuated throughout the experiment and reached the highest value. The overall trend indicates variations in buffering capability which might alter the pH environment during CO_2 electrochemical reduction.

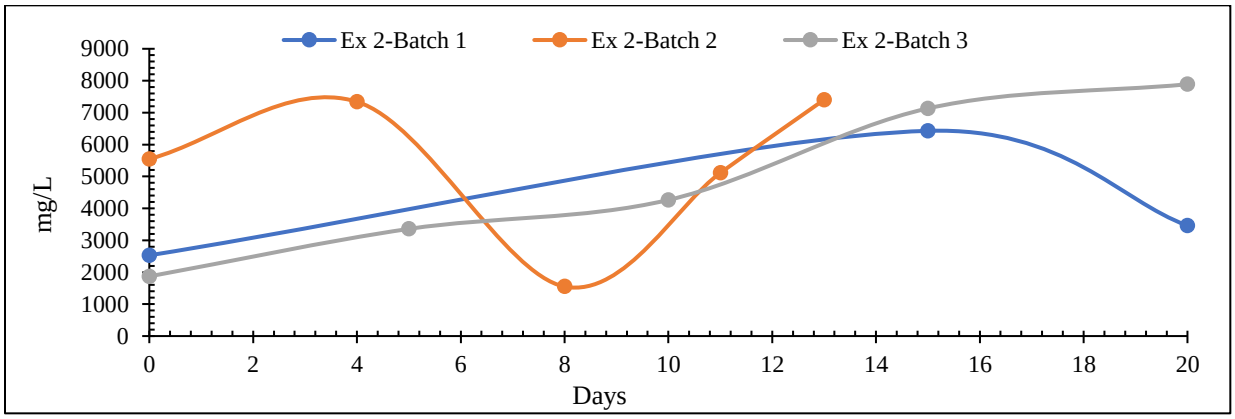

Figure 4.7 Alkalinity ($CaCO_3$) in a different time interval during CO_2 electroreduction into CH_4.

4.2.5 COD evaluation

When converting CO_2 electrochemically, organic substrates that contribute to COD are used as a source of biocatalyst, which is frequently derived from microbes. Electron transfer processes impact the electron balance during the metabolic activity of the biocatalyst. Redox potential is impacted by this activity, which in turn influences electrode reactions and CO_2 reduction pathways efficiency. Acidic or basic byproducts that the biocatalyst produces or consumes may affect the pH of the solution and electrochemical reactions. Hence, the evaluation of total COD (**Figure 4.8**) and soluble COD (**Figure 4.9**) offers an understanding of substrate availability, dynamic interactions, and possible synergies within the system of each batch experiment. The COD value fluctuated in the electrochemical experiment which indicated changes in the amount of organic material. An increase in total-COD suggested the presence or production of organic substrates, which might be the outcome of CO_2 electrochemically converting to organic molecules. The soluble organic species, possible intermediates, or byproducts of CO_2 reduction were reflected in changes in soluble-COD. These significant variations in COD may be related to the generation of CH4. Increased organic content, as demonstrated by total-COD, may provide more carbon sources for effective electrochemical conversion of CO_2 to CH_4. Moreover, the variations in soluble-COD and total-COD highlight the reactivity with organic molecules, which affects CO_2 conversion efficiency and selectivity. Besides, the effective mass transfer of CO_2 to the electrode surface is essential, and high COD levels may affect it. Several reduction pathways can be influenced by the presence of additional organic species, which can affect how distinct products are formed. Selectivity in the electrochemical process might be influenced by this complex interaction of COD fluctuations. In addition, COD analysis is also important for the environment since it may be used to estimate the possible emission of organic and inorganic contaminants. Assessing the impact on

the environment of the electrochemical CO_2 conversion process is made easier with a recognition of the COD profile. This detailed study provides on the complex interplay between COD changes and the effectiveness and selectivity of CO_2 electroreduction into CH_4.

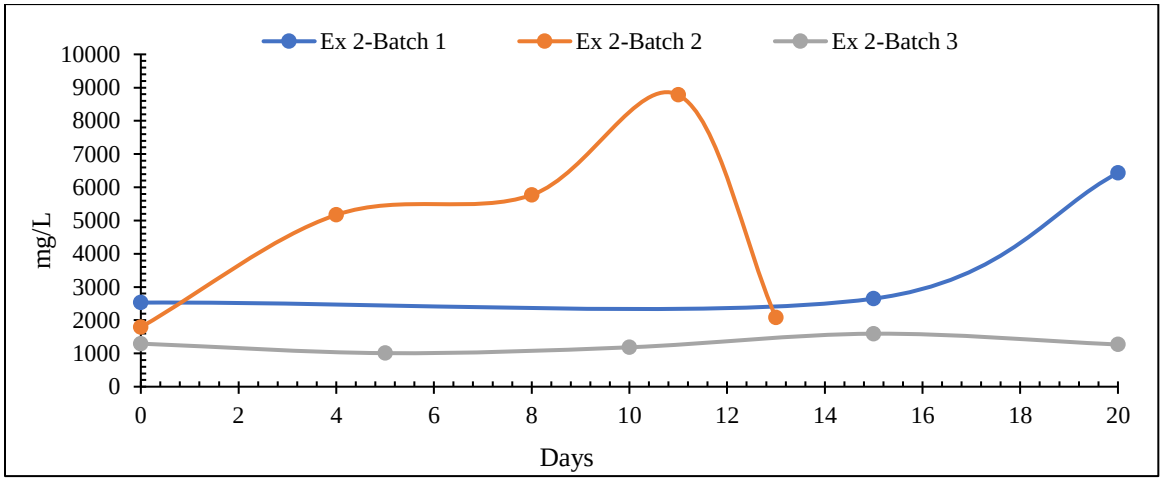

Figure 4.8 Total COD variation during methanogenesis.

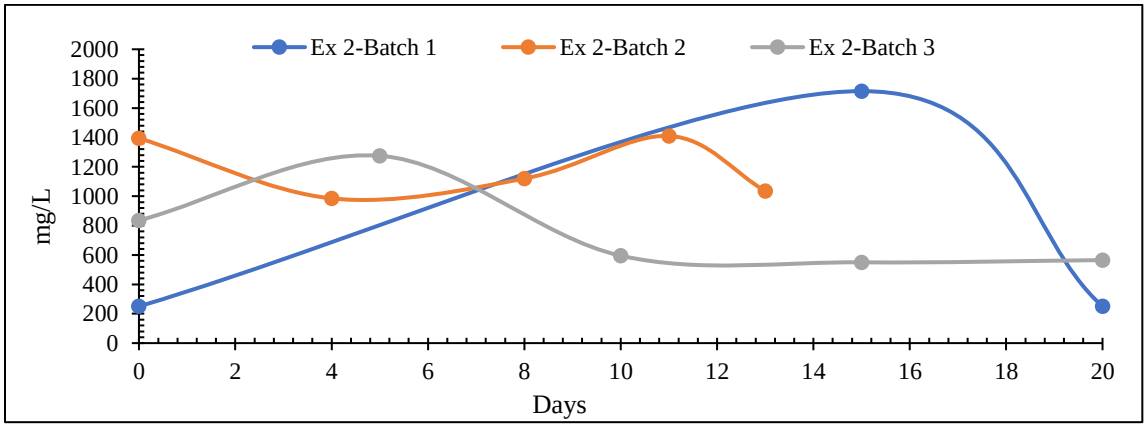

Figure 4.9 Soluble COD variation during methanogenesis.

4.2.6 VFAs analysis

VFAs are intermediate chemicals formed during anaerobic digestion processes that indicate organic matter breakdown during CO_2 reduction into CH_4. A substantial amount of specific VFAs, such as butyric acid (**Figure 4.10**) and propionic acid (**Figure 4.11**), might indicate greater

substrate availability for methanogenic microbial activities, thus driving higher CH_4 generation. In Ex 2-Batch 1, n-valeric acid was found at 0.72 mg/L after 15 days while acetic acid produced higher after 20 days (**Figure 4.12**). Further, the isovaleric acid concentration fluctuated over time (**Figure 4.13**). In Ex 2-Batch 2, isobutyric acid formed after 4 and 8 days (**Figure 4.14**) as well as isocaproic acid and heptanoic acid generated in a certain time interval (**Figure 4.15**). The fluctuations in VFA concentrations, notably the rise and fall in specific acids across different time points, might indicate varying stages of microbial activity or shifts in the metabolic pathways involved in CH_4 generation. The decline in VFAs followed by subsequent increases could relate to changes in the availability of substrates for methanogenesis, influencing CH_4 production rates during CO_2 reduction. Moreover, CNTs enhance butyrate conversion to CH_4 in syntrophic coculture, demonstrating its positive impact on specific microbial interactions [125]. The observed total VFAs variations in the findings refer to the dynamic nature of the organic compound breakdown and its possible influence on microbial activities involved in CH_4 synthesis during electrochemical CO_2 reduction. Ex 2-Batch 3 shows a reduction in soluble-COD compared to its initial value, which is likely due to microbial growth consuming soluble-COD. Further, no VFAs are accumulated in Ex 2-Batch 3, and the reduction in the amount of acetic acid which is easily converted to CH_4, indicates anaerobic digestion. The electrochemical acetic acid oxidation is inhibited by the presence of a separate cathode, indicating that anaerobic digestion may contribute to some of the CH_4 generation. Moreover, the presence of propionic acid and isovaleric acid in Ex 2-Batch 1 as well as the rise in soluble-COD might be related to chemical processes occurring inside the system.

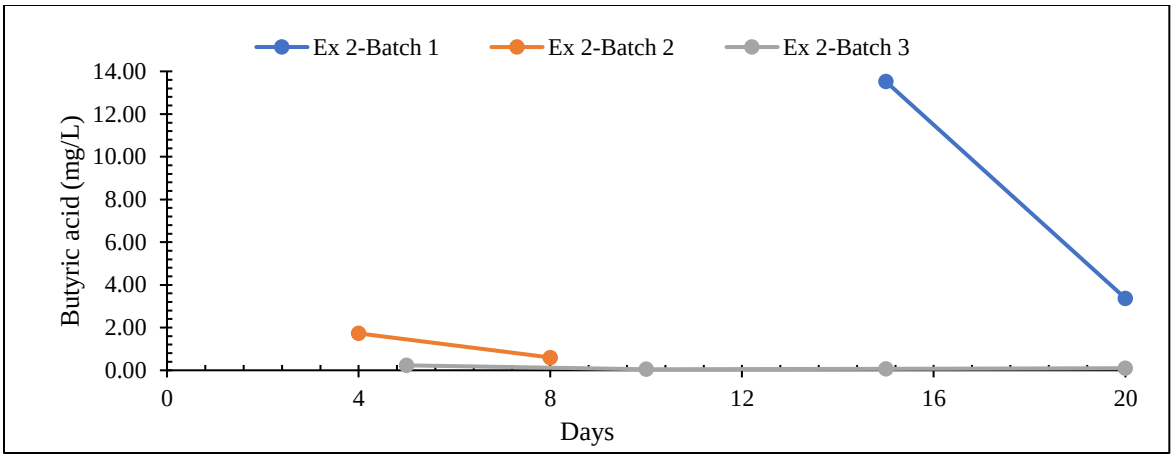

Figure 4.10 Butyric acid concentration during methanogenic microbial activities.

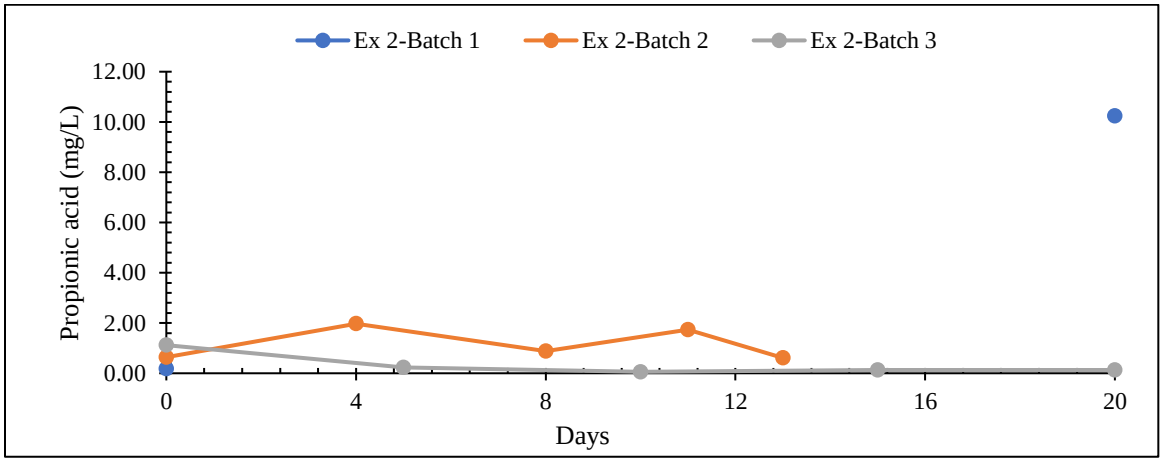

Figure 4.11 Propionic acid concentration during methanogenic microbial activities.

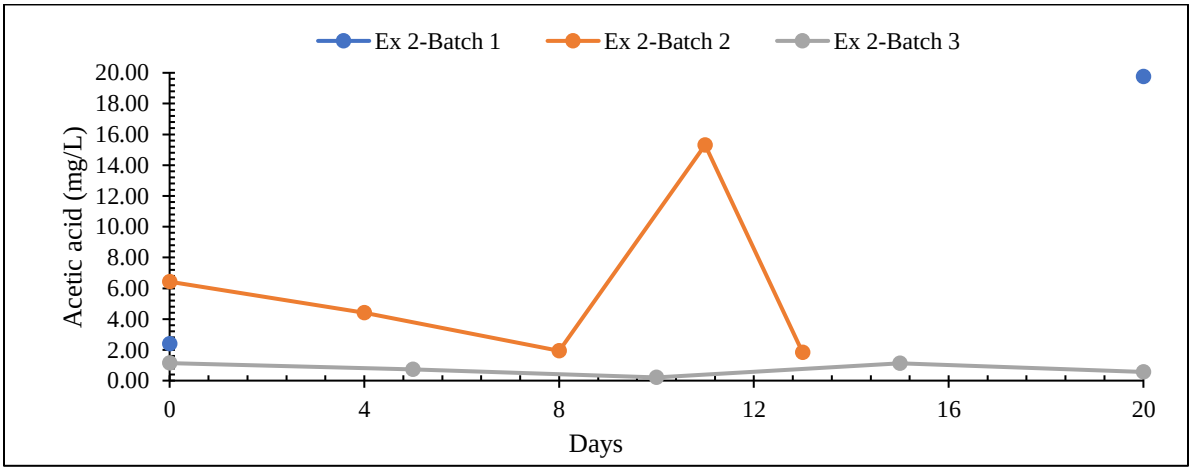

Figure 4.12 Acetic acid concentration during methanogenic microbial activities.

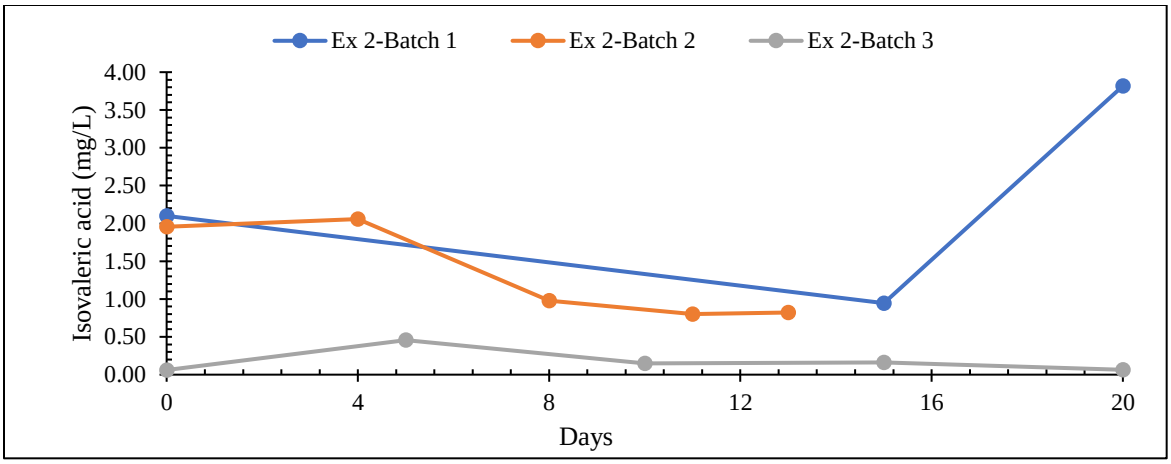

Figure 4.13 Isovaleric acid concentration during methanogenic microbial activities.

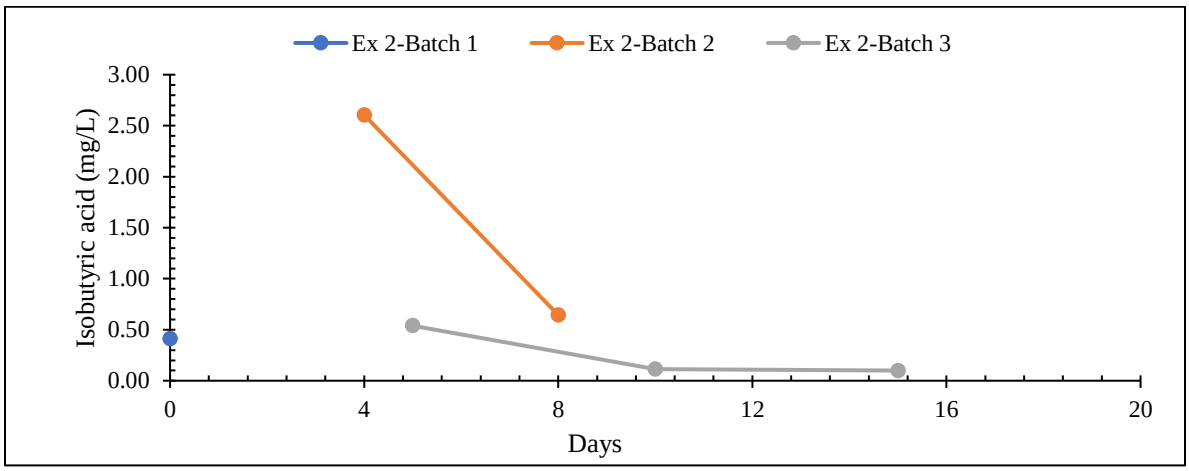

Figure 4.14 Isobutyric acid concentration during methanogenic microbial activities.

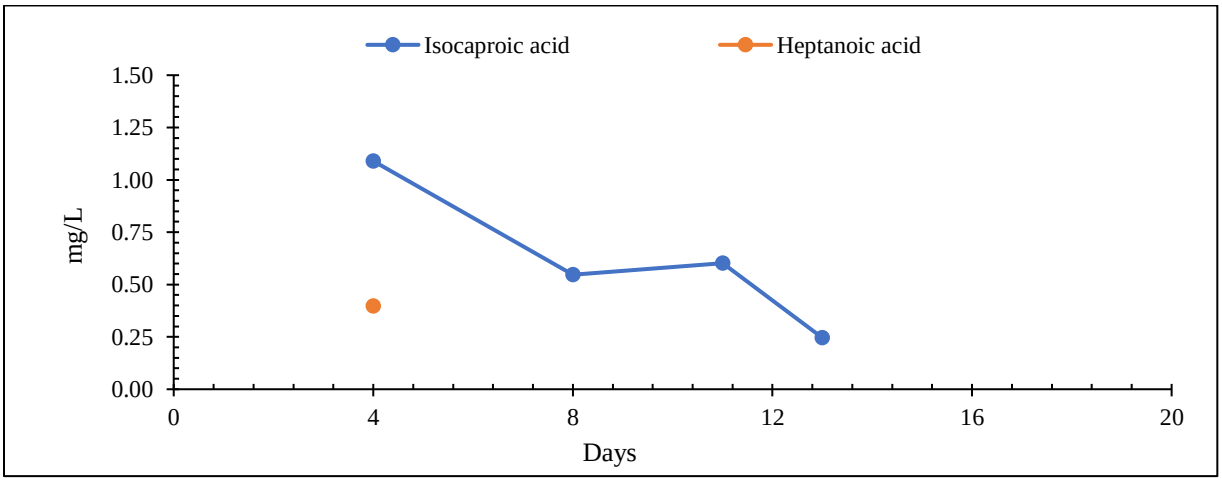

Figure 4.15 Isocaproic and heptanoic acid concentration in Ex 2-Batch 2.

4.3 Electrodes characterization

The CNTs on the aluminum substrate were distributed uniformly on the three-dimensional smooth surface. The surface morphology exhibited an arrangement of aligned nanotubes that possessed a certain range of diameter consistency as shown by four different dimensions of electrodes in **Figure 4.16, 4.17, 4.18, and 4.19**, among other significant characteristics. The images obtained from the SEM clearly showed that CNTs were effectively deposited onto the pre-sputtered aluminum thin foils coated with Ni, exhibiting uniformity and adherence throughout the electrode surface. The Ni catalyst was chosen due to its more effective performance in producing CNTs [134], [135], [136]. A smooth surface was observed after coating with Ni catalyst, which is related to the binding of Ni catalyst over the activated carbon surface [33]. Moreover, the contact between the carbon nanotubes and the aluminum substrate was also clarified by the SEM investigation. It revealed an effective interfacial connection, providing the structural stability required for subsequent electrochemical investigations. The SEM analysis revealed the uniformity and integrity of the CNTs layer, which is vital to enabling effective CO_2 reduction reactions on the electrode surface.

Furthermore, the efficiency of the CVD process in producing evenly distributed and well-aligned carbon nanotubes on the aluminum substrate was confirmed by the SEM observations. These focused on the relationship between the variables that changed during the CVD process such as gas ratio, flow rates, and duration, and whether those variables affected the distribution and shape of the synthesized CNTs. The CVD approach was preferred because it offered a 90% CNTs yield and allowed for the growth of highly pure CNTs [137], [138]. This association configures the stage for a potential electrochemical study to maximize CO_2 reduction efficiency by providing insight into the way modifications in these factors affect the structural properties of the electrode.

Additionally, several carbon sources can be used to support the formation of CNTs, such as ethylene (C_2H_4), acetylene (C_2H_2), and methane (CH_4) [137], [138]. However, C_2H_2 was selected because it performs more effectively than activated carbon in promoting the formation of CNTs [136]. The length of time and amount of acetylene supplied had significant effects on CNTs development. Research has shown that a higher quantity of C_2H_2 supply was efficient in facilitating the development of a well-structured film, emphasizing the need to preserve a constant and reliable supply for ideal growth and film formation [136].

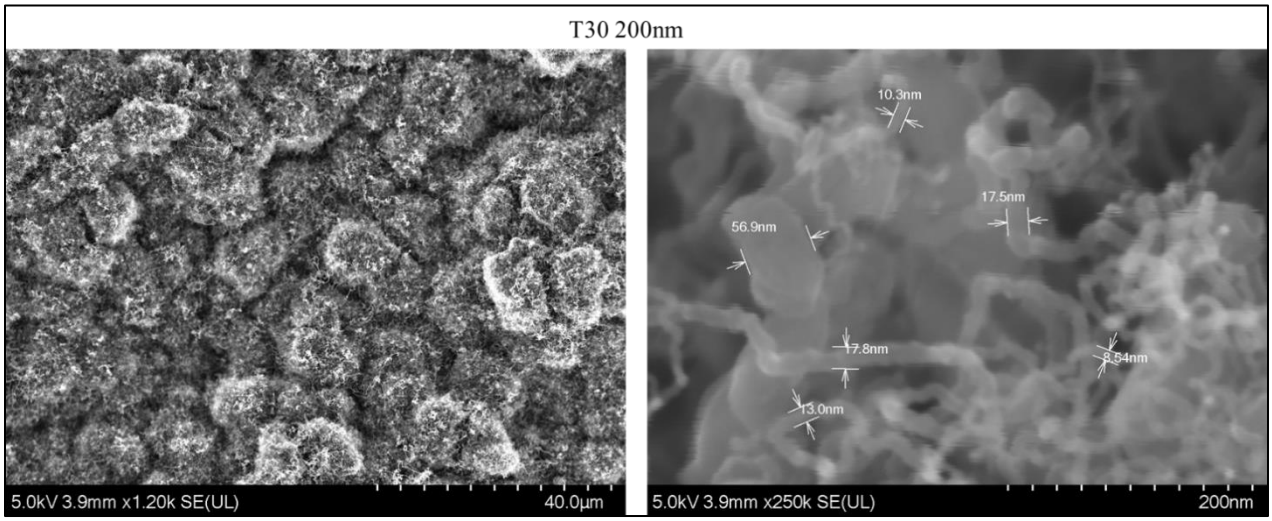

Figure 4.16 SEM image of 200 nm Al/CNTs electrode.

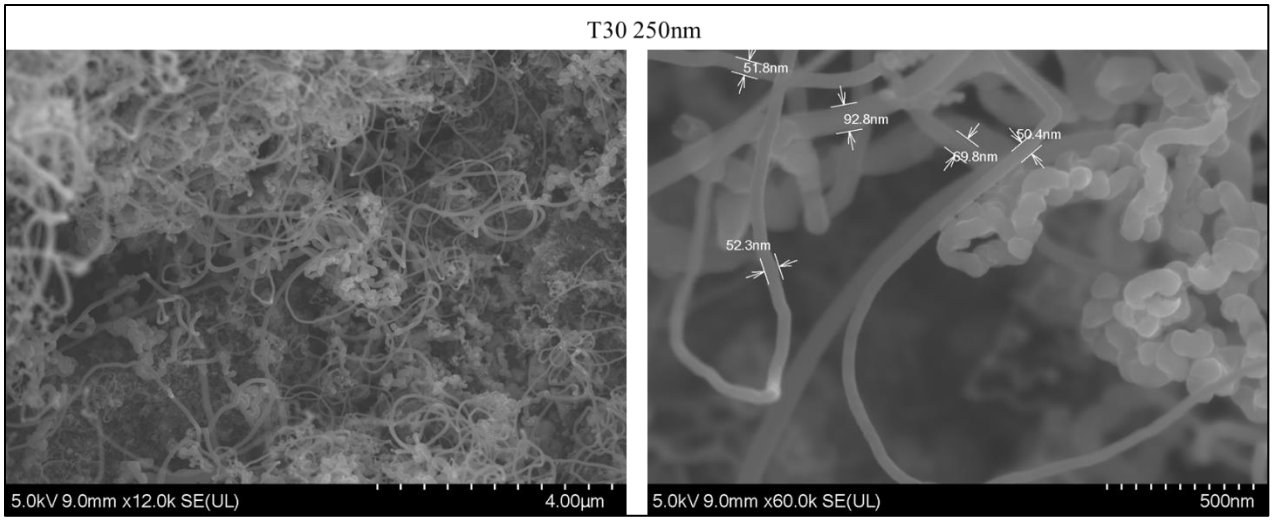

Figure 4.17 SEM image of 250 nm Al/CNTs electrode.

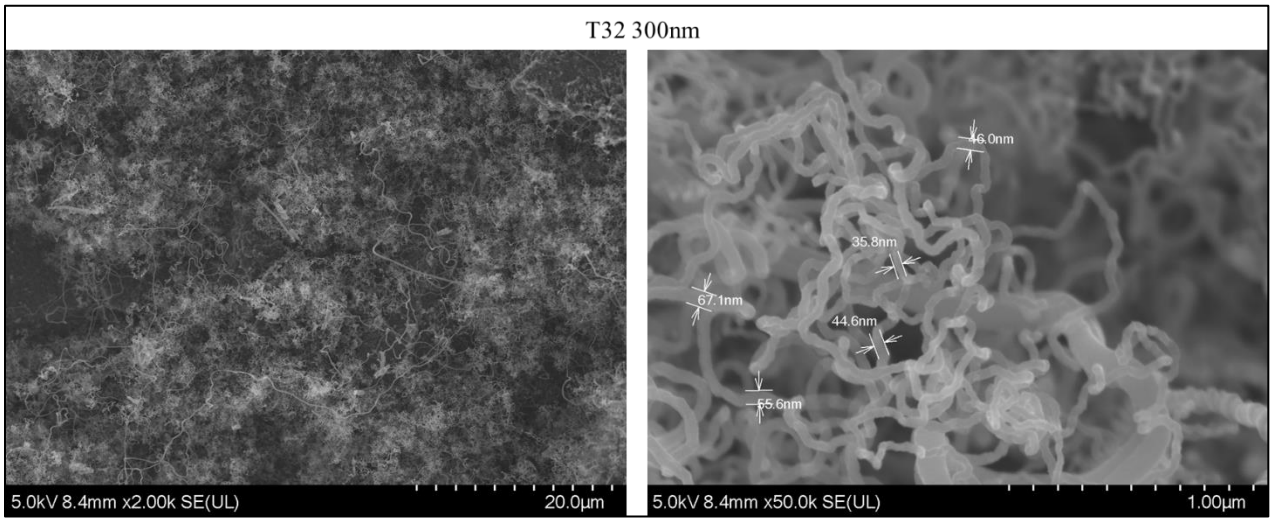

Figure 4.18 SEM image of 300 nm Al/CNTs electrode.

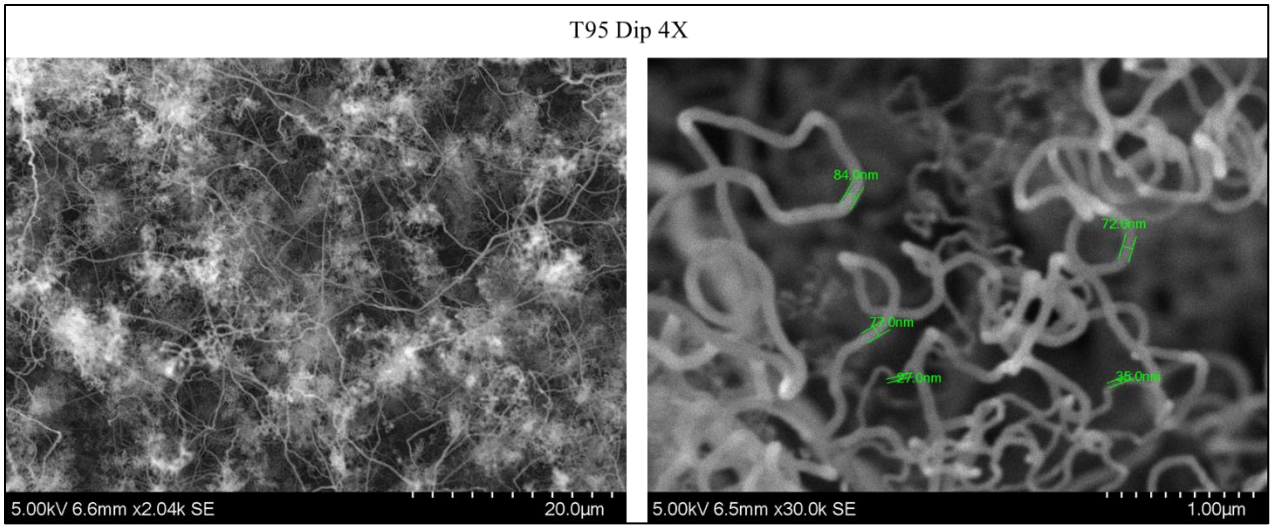

Figure 4.19 SEM image of Al/CNTs electrode.

4.4 Limitations

The variations in fabrication quality were introduced when Al/CNTs electrodes were obtained from external sources. The absence of internal control made it difficult to ensure electrode stability. An additional spatial variable was introduced when the biocatalyst was incorporated after 10 days, which might affect the electrochemical results and affect microbial adaptability. A thorough assessment of long-term stability was hampered by the partial failure of the working electrode that occurred during Ex 2-Batch 2 which restricts the continuing analysis of data. When CH_4 production inhibited under specific conditions, the effectiveness of the system or the impact of various potential factors on CH_4 generation was examined. Even while SEM imaging was beneficial, it can be impacted by external laboratory techniques.

5 Conclusion

This chapter describes the summary and future recommendations of the thesis experiment with the utilization of Al/CNTs electrodes for CO_2 reduction into CH_4 was an emerging advancement in electrochemical research using biocatalyst, supported by thorough studies such as total-COD, soluble-COD, VFAs analysis, alkalinity test, SEM imaging, current generation, and GC analysis. Moreover, the productivity and sustainability of the electrochemical CO_2 conversion process for CH_4 generation were significantly revealed by the observed production efficiencies, which include CO_2 conversion efficiency, Faradic efficiency, and energy efficiency.

5.1 Summary

The electrochemical study revealed substantial progress in biogas production through effective CO_2 conversion on Al/CNTs electrodes by using microbial catalysts. In Ex 2-Batch 1, the production of 0.34 mL/(cm^2 Al/CNTs surface area) was observed over 10 days without yeast extract, while significant production reached 1.49 mL/(cm^2 Al/CNTs surface area) with yeast extract. The associated CO_2 conversion efficiency, Faradic efficiency, and energy efficiency were 8.47%, 9.67%, and 1.64%, respectively, at a current density of -0.346 mA/cm^2. In Ex 2-Batch 2, a remarkable increase to 0.69 mL/(cm^2 Al/CNTs surface area) over 8 days exhibited enhanced CO_2 conversion, with Faradic efficiency, and energy efficiency of 14.10%, 31.26%, and 5.30% with -0.062 mA/cm^2 current density, respectively. Finally, in Ex 2-Batch 3, a considerable biogas production of 3.66 mL/(cm^2 Al/CNTs surface area) over 20 days demonstrated efficient CO_2 conversion, yielding efficiencies of 18.53%, 18.39%, and 3.12%, respectively, at a current density of -0.488 mA/cm^2.

5.2 Recommendations

The limited focus on CH_4 synthesis prevented other possible reduction products from being explored, which impeded the development of adequate knowledge of electrochemical pathways. The analysis of soluble-COD and VFAs findings indicates the absence of usual VFAs which implies the need to research the production of alternative chemicals, with a focus on exploring possible chemical pathways in the electrochemical CO_2 reduction process. Moreover, the CO_2 bubbler saturation experiment was used to increase the solubility of CO_2 in liquid. However, the injection of CO_2 into the headspace without bubbling in the electrochemical reactor can result in a lack of CO_2 flow. Therefore, considering the continuous flow processes of CO_2 flow with recirculation simultaneous with the electrochemical CO_2 reduction process can be recommended to address this aspect in future reactor design to enhance the efficiency of the process for biomethane production. This design can be implemented and requires further investigation of the state-of-the-art electrochemical biogas upgrading system with a continuous flow of biogas into the reactor cell. Additionally, characterizing the Al/CNTs electrode using methods such as cyclic voltammetry or electrochemical impedance spectroscopy can provide observations on the longevity of electrodes in various conditions, allowing for further investigation and modification.

References

[1] S. J. Davis, K. Caldeira, and H. D. Matthews, 'Future CO_2 Emissions and Climate Change from Existing Energy Infrastructure', *Science (1979)*, vol. 329, no. 5997, pp. 1330–1333, Sep. 2010, doi: 10.1126/science.1188566.

[2] O. Hoegh-Guldberg *et al.*, 'Coral Reefs Under Rapid Climate Change and Ocean Acidification', *Science (1979)*, vol. 318, no. 5857, pp. 1737–1742, Dec. 2007, doi: 10.1126/science.1152509.

[3] G. Pasternak, P. Rutkowski, E. Śliwka, B. Kołwzan, and J. Rybak, 'Broad Coal Tar Biodegradative Potential of Rhodococcus erythropolis B10 Strain Isolated from Former Gasworks Site', *Water Air Soil Pollut*, vol. 214, no. 1, pp. 599–608, 2011, doi: 10.1007/s11270-010-0449-2.

[4] H. Ritchie, M. Roser, and P. Rosado, 'CO_2 and Greenhouse Gas Emissions', *Our World in Data*, 2020, Accessed: Oct. 17, 2023. [Online]. Available: https://ourworldindata.org/co2-and-greenhouse-gas-emissions

[5] J. L. Holechek, H. M. E. Geli, M. N. Sawalhah, and R. Valdez, 'A Global Assessment: Can Renewable Energy Replace Fossil Fuels by 2050?', *Sustainability (Switzerland)*, vol. 14, no. 8, Apr. 2022, doi: 10.3390/su14084792.

[6] A. Kalair, N. Abas, M. S. Saleem, A. R. Kalair, and N. Khan, 'Role of energy storage systems in energy transition from fossil fuels to renewables', *Energy Storage*, vol. 3, no. 1, p. e135, Feb. 2021, doi: https://doi.org/10.1002/est2.135.

[7] D. J. Soeder, 'Fossil Fuels and Climate Change', in *Fracking and the Environment: A scientific assessment of the environmental risks from hydraulic fracturing and fossil fuels*, D. J. Soeder, Ed., Cham: Springer International Publishing, 2021, pp. 155–185. doi: 10.1007/978-3-030-59121-2_9.

[8] E. Dogan, M. T. Majeed, and T. Luni, 'Revisiting the nexus of ecological footprint, unemployment, and renewable and non-renewable energy for South Asian economies: Evidence from novel research methods', *Renew Energy*, vol. 194, pp. 1060–1070, 2022, doi: https://doi.org/10.1016/j.renene.2022.05.165.

[9] A. Sharif, O. Baris-Tuzemen, G. Uzuner, I. Ozturk, and A. Sinha, 'Revisiting the role of renewable and non-renewable energy consumption on Turkey's ecological footprint: Evidence from Quantile ARDL approach', *Sustain Cities Soc*, vol. 57, p. 102138, Jun. 2020, doi: 10.1016/J.SCS.2020.102138.

[10] S. Hernández, M. Amin Farkhondehfal, F. Sastre, M. Makkee, G. Saracco, and N. Russo, 'Syngas production from electrochemical reduction of CO_2: current status and prospective implementation', *Green Chemistry*, vol. 19, no. 10, pp. 2326–2346, 2017, doi: 10.1039/C7GC00398F.

[11] G. Pasternak, 'Electrochemical approach for biogas upgrading', *Emerging Technologies and Biological Systems for Biogas Upgrading*, pp. 223–254, Jan. 2021, doi: 10.1016/B978-0-12-822808-1.00009-X.

[12] N. Aryal and T. Kvist, 'Alternative of Biogas Injection into the Danish Gas Grid System—A Study from Demand Perspective', *ChemEngineering*, vol. 2, no. 3, 2018, doi: 10.3390/chemengineering2030043.

[13] N. Aryal, T. Kvist, F. Ammam, D. Pant, and L. D. M. Ottosen, 'An overview of microbial biogas enrichment', *Bioresour Technol*, vol. 264, pp. 359–369, 2018, doi: https://doi.org/10.1016/j.biortech.2018.06.013.

[14] Z. Liu *et al.*, 'States and challenges for high-value biohythane production from waste biomass by dark fermentation technology', *Bioresour Technol*, vol. 135, pp. 292–303, 2013, doi: https://doi.org/10.1016/j.biortech.2012.10.027.

[15] Y. Li *et al.*, 'Composition and Toxicity of Biogas Produced from Different Feedstocks in California', *Environ Sci Technol*, vol. 53, no. 19, pp. 11569–11579, Oct. 2019, doi: 10.1021/acs.est.9b03003.

[16] T. Kvist and N. Aryal, 'Methane loss from commercially operating biogas upgrading plants', *Waste Management*, vol. 87, pp. 295–300, 2019, doi: https://doi.org/10.1016/j.wasman.2019.02.023.

[17] N. Aryal, L. D. M. Ottosen, M. V. W. Kofoed, and D. Pant, *Emerging Technologies and Biological Systems for Biogas Upgrading*. Academic Press, 2021. doi: http://dx.doi.org/10.1016/C2019-0-01200-9.

[18] I. Angelidaki *et al.*, 'Biogas upgrading and utilization: Current status and perspectives', *Biotechnol Adv*, vol. 36, no. 2, pp. 452–466, 2018, doi: https://doi.org/10.1016/j.biotechadv.2018.01.011.

[19] S. Fu, I. Angelidaki, and Y. Zhang, 'In situ Biogas Upgrading by CO_2-to-CH_4 Bioconversion', *Trends Biotechnol*, vol. 39, no. 4, pp. 336–347, 2021, doi: 10.1016/j.tibtech.2020.08.006.

[20] N. Aryal, Y. Zhang, S. Bajracharya, D. Pant, and X. Chen, 'Microbial electrochemical approaches of carbon dioxide utilization for biogas upgrading', *Chemosphere*, vol. 291, p. 132843, 2022, doi: https://doi.org/10.1016/j.chemosphere.2021.132843.

[21] C. Song, 'CO_2 Conversion and Utilization: An Overview', in *CO_2 Conversion and Utilization*, vol. 809, in ACS Symposium Series, vol. 809. , American Chemical Society, 2002, pp. 2–30. doi: doi:10.1021/bk-2002-0809.ch001.

[22] Z. Huang, L. Lu, D. Jiang, D. Xing, and Z. J. Ren, 'Electrochemical hythane production for renewable energy storage and biogas upgrading', *Appl Energy*, vol. 187, pp. 595–600, 2017, doi: https://doi.org/10.1016/j.apenergy.2016.11.099.

[23] H. T. Ahangari, T. Portail, and A. T. Marshall, 'Comparing the electrocatalytic reduction of CO_2 to CO on gold cathodes in batch and continuous flow electrochemical cells', *Electrochem commun*, vol. 101, pp. 78–81, 2019, doi: https://doi.org/10.1016/j.elecom.2019.03.005.

[24] N. S. Spinner, J. A. Vega, and W. E. Mustain, 'Recent progress in the electrochemical conversion and utilization of CO_2', *Cite this: Catal. Sci. Technol*, vol. 2, pp. 19–28, 2012, doi: 10.1039/c1cy00314c.

[25] D. T. Whipple and P. J. A. Kenis, 'Prospects of CO_2 Utilization via Direct Heterogeneous Electrochemical Reduction', *J Phys Chem Lett*, vol. 1, no. 24, pp. 3451–3458, Dec. 2010, doi: 10.1021/jz1012627.

[26] C. F. C. Lim, D. A. Harrington, and A. T. Marshall, 'Effects of mass transfer on the electrocatalytic CO_2 reduction on Cu', *Electrochim Acta*, vol. 238, pp. 56–63, 2017, doi: https://doi.org/10.1016/j.electacta.2017.04.017.

[27] N. Gupta, M. Gattrell, and B. MacDougall, 'Calculation for the cathode surface concentrations in the electrochemical reduction of CO_2 in $KHCO_3$ solutions', *J Appl Electrochem*, vol. 36, no. 2, pp. 161–172, 2006, doi: 10.1007/s10800-005-9058-y.

[28] M. Azuma, K. Hashimoto, M. Hiramoto, M. Watanabe, and T. Sakata, 'Electrochemical Reduction of Carbon Dioxide on Various Metal Electrodes in Low-Temperature Aqueous $KHCO_3$ Media', *J Electrochem Soc*, vol. 137, no. 6, pp. 1772–1778, Jun. 1990, doi: 10.1149/1.2086796.

[29] C. F. C. Lim, D. A. Harrington, and A. T. Marshall, 'Altering the selectivity of galvanostatic CO_2 reduction on Cu cathodes by periodic cyclic voltammetry and potentiostatic steps', *Electrochim Acta*, vol. 222, pp. 133–140, 2016, doi: https://doi.org/10.1016/j.electacta.2016.10.185.

[30] J. Lee and Y. Tak, 'Electrocatalytic activity of Cu electrode in electroreduction of CO_2', *Electrochim Acta*, vol. 46, no. 19, pp. 3015–3022, 2001, doi: https://doi.org/10.1016/S0013-4686(01)00527-8.

[31] P. Gahlot *et al.*, 'Conductive material engineered direct interspecies electron transfer (DIET) in anaerobic digestion: Mechanism and application', *Environ Technol Innov*, vol. 20, p. 101056, 2020, doi: https://doi.org/10.1016/j.eti.2020.101056.

[32] Y. Dang, D. Sun, T. L. Woodard, L.-Y. Wang, K. P. Nevin, and D. E. Holmes, 'Stimulation of the anaerobic digestion of the dry organic fraction of municipal solid waste (OFMSW) with carbon-based conductive materials', *Bioresour Technol*, vol. 238, pp. 30–38, 2017, doi: https://doi.org/10.1016/j.biortech.2017.04.021.

[33] N. Aryal, L. Feng, S. Wang, and X. Chen, 'Surface-modified activated carbon for anaerobic digestion to optimize the microbe-material interaction', *Science of The Total Environment*, vol. 886, p. 163985, 2023, doi: https://doi.org/10.1016/j.scitotenv.2023.163985.

[34] N. Aryal, F. Ammam, S. A. Patil, and D. Pant, 'An overview of cathode materials for microbial electrosynthesis of chemicals from carbon dioxide', *Green Chem.*, vol. 19, no. 24, pp. 5748–5760, 2017, doi: 10.1039/C7GC01801K.

[35] N. Elgrishi, K. J. Rountree, B. D. McCarthy, E. S. Rountree, T. T. Eisenhart, and J. L. Dempsey, 'A Practical Beginner's Guide to Cyclic Voltammetry', *J Chem Educ*, vol. 95, no. 2, pp. 197–206, Feb. 2018, doi: 10.1021/acs.jchemed.7b00361.

[36] W. An, J. K. Hong, P. N. Pintauro, K. Warner, and W. Neff, 'The electrochemical hydrogenation of edible oils in a solid polymer electrolyte reactor. I. Reactor design and operation', *J Am Oil Chem Soc*, vol. 75, no. 8, pp. 917–925, 1998, doi: 10.1007/s11746-998-0267-5.

[37] D. Bagchi, S. Roy, S. Ch. Sarma, and S. C. Peter, 'Toward Unifying the Mechanistic Concepts in Electrochemical CO_2 Reduction from an Integrated Material Design and Catalytic Perspective', *Adv Funct Mater*, vol. 32, no. 51, p. 2209023, Dec. 2022, doi: https://doi.org/10.1002/adfm.202209023.

[38] R. A. Tufa *et al.*, 'Towards highly efficient electrochemical CO_2 reduction: Cell designs, membranes and electrocatalysts', *Appl Energy*, vol. 277, p. 115557, 2020, doi: https://doi.org/10.1016/j.apenergy.2020.115557.

[39] N. Ali, M. Bilal, M. S. Nazir, A. Khan, F. Ali, and H. M. N. Iqbal, 'Thermochemical and electrochemical aspects of carbon dioxide methanation: A sustainable approach to generate fuel via waste to energy theme', *Science of The Total Environment*, vol. 712, p. 136482, 2020, doi: https://doi.org/10.1016/j.scitotenv.2019.136482.

[40] S. Zeng *et al.*, 'Electrochemical promoted dry methane reforming for power and syngas co-generation in solid oxide fuel cells: Experiments, modelling and optimizations', *Int J Hydrogen Energy*, 2023, doi: https://doi.org/10.1016/j.ijhydene.2023.10.151.

[41] C. Chen, J. F. Khosrowabadi Kotyk, and S. W. Sheehan, 'Progress toward Commercial Application of Electrochemical Carbon Dioxide Reduction', *Chem*, vol. 4, no. 11, pp. 2571–2586, 2018, doi: https://doi.org/10.1016/j.chempr.2018.08.019.

[42] J. Na *et al.*, 'General technoeconomic analysis for electrochemical coproduction coupling carbon dioxide reduction with organic oxidation', *Nat Commun*, vol. 10, no. 1, p. 5193, 2019, doi: 10.1038/s41467-019-12744-y.

[43] L. Daniels, N. Belay, B. S. Rajagopal, and P. J. Weimer, 'Bacterial Methanogenesis and Growth from CO_2 with Elemental Iron as the Sole Source of Electrons', *Science (1979)*, vol. 237, no. 4814, pp. 509–511, Jul. 1987, doi: 10.1126/science.237.4814.509.

[44] S. Cheng, D. Xing, D. F. Call, and B. E. Logan, 'Direct Biological Conversion of Electrical Current into Methane by Electromethanogenesis', *Environ Sci Technol*, vol. 43, no. 10, pp. 3953–3958, May 2009, doi: 10.1021/es803531g.

[45] B. Zhou *et al.*, 'Highly efficient binary copper−iron catalyst for photoelectrochemical carbon dioxide reduction toward methane', *Proceedings of the National Academy of Sciences*, vol. 117, no. 3, pp. 1330–1338, Jan. 2020, doi: 10.1073/pnas.1911159117.

[46] S. Mou *et al.*, 'Boron Phosphide Nanoparticles: A Nonmetal Catalyst for High-Selectivity Electrochemical Reduction of CO_2 to CH_3OH', *Advanced Materials*, vol. 31, no. 36, p. 1903499, Sep. 2019, doi: https://doi.org/10.1002/adma.201903499.

[47] S. Furukawa, M. Okada, and Y. Suzuki, 'Isolation of Oxygen Formed during Catalytic Reduction of Carbon Dioxide Using a Solid Electrolyte Membrane', *Energy & Fuels*, vol. 13, no. 5, pp. 1074–1081, Sep. 1999, doi: 10.1021/ef990039t.

[48] A. J. Bard, L. R. Faulkner, and H. S. White, *Electrochemical methods: fundamentals and applications*. John Wiley & Sons, 2022.

[49] M.-J. Cheng, E. L. Clark, H. H. Pham, A. T. Bell, and M. Head-Gordon, 'Quantum Mechanical Screening of Single-Atom Bimetallic Alloys for the Selective Reduction of CO_2 to C_1 Hydrocarbons', *ACS Catal*, vol. 6, no. 11, pp. 7769–7777, Nov. 2016, doi: 10.1021/acscatal.6b01393.

[50] M. G. Kibria *et al.*, 'Electrochemical CO_2 Reduction into Chemical Feedstocks: From Mechanistic Electrocatalysis Models to System Design', *Advanced Materials*, vol. 31, no. 31, p. 1807166, Aug. 2019, doi: https://doi.org/10.1002/adma.201807166.

[51] D. Ren, J. Fong, and B. S. Yeo, 'The effects of currents and potentials on the selectivities of copper toward carbon dioxide electroreduction', *Nat Commun*, vol. 9, no. 1, p. 925, 2018, doi: 10.1038/s41467-018-03286-w.

[52] H. Zhang *et al.*, 'Computational and experimental demonstrations of one-pot tandem catalysis for electrochemical carbon dioxide reduction to methane', *Nat Commun*, vol. 10, no. 1, p. 3340, 2019, doi: 10.1038/s41467-019-11292-9.

[53] A. A. Peterson and J. K. Nørskov, 'Activity Descriptors for CO_2 Electroreduction to Methane on Transition-Metal Catalysts', *J Phys Chem Lett*, vol. 3, no. 2, pp. 251–258, Jan. 2012, doi: 10.1021/jz201461p.

[54] W. Xu, Y. Qiu, T. Zhang, X. Li, and H. Zhang, 'The Effect of Organic Additives on the Activity and Selectivity of CO_2 Electroreduction: The Role of Functional Groups', *ChemSusChem*, vol. 11, no. 17, pp. 2904–2911, Sep. 2018, doi: https://doi.org/10.1002/cssc.201801458.

[55] K. Jiang *et al.*, 'Metal ion cycling of Cu foil for selective C–C coupling in electrochemical CO_2 reduction', *Nat Catal*, vol. 1, no. 2, pp. 111–119, 2018, doi: 10.1038/s41929-017-0009-x.

[56] G. Wang, J. Pan, S. P. Jiang, and H. Yang, 'Gas phase electrochemical conversion of humidified CO_2 to CO and H_2 on proton-exchange and alkaline anion-exchange

membrane fuel cell reactors', *Journal of CO2 Utilization*, vol. 23, pp. 152–158, 2018, doi: https://doi.org/10.1016/j.jcou.2017.11.010.

[57] P. De Luna *et al.*, 'Catalyst electro-redeposition controls morphology and oxidation state for selective carbon dioxide reduction', *Nat Catal*, vol. 1, no. 2, pp. 103–110, 2018, doi: 10.1038/s41929-017-0018-9.

[58] H. Lv *et al.*, 'Infiltration of $Ce_{0.8}Gd_{0.2}O_{1.9}$ nanoparticles on $Sr_2Fe_{1.5}Mo_{0.5}O_{6-\delta}$ cathode for CO_2 electroreduction in solid oxide electrolysis cell', *Journal of Energy Chemistry*, vol. 35, pp. 71–78, 2019, doi: https://doi.org/10.1016/j.jechem.2018.11.002.

[59] E. L. Clark and A. T. Bell, 'Direct Observation of the Local Reaction Environment during the Electrochemical Reduction of CO_2', *J Am Chem Soc*, vol. 140, no. 22, pp. 7012–7020, Jun. 2018, doi: 10.1021/jacs.8b04058.

[60] M. Lee, C. Nagendranatha Reddy, and B. Min, 'In situ integration of microbial electrochemical systems into anaerobic digestion to improve methane fermentation at different substrate concentrations', *Int J Hydrogen Energy*, vol. 44, no. 4, pp. 2380–2389, 2019, doi: https://doi.org/10.1016/j.ijhydene.2018.08.051.

[61] X.-Z. Fu *et al.*, 'A single microbial electrochemical system for CO_2 reduction and simultaneous biogas purification, upgrading and sulfur recovery', *Bioresour Technol*, vol. 297, p. 122448, 2020, doi: https://doi.org/10.1016/j.biortech.2019.122448.

[62] S. Y. Liu, W. Charles, G. Ho, R. Cord-Ruwisch, and K. Y. Cheng, 'Bioelectrochemical enhancement of anaerobic digestion: Comparing single- and two-chamber reactor configurations at thermophilic conditions', *Bioresour Technol*, vol. 245, pp. 1168–1175, 2017, doi: https://doi.org/10.1016/j.biortech.2017.08.095.

[63] M. Murto, L. Björnsson, and B. Mattiasson, 'Impact of food industrial waste on anaerobic co-digestion of sewage sludge and pig manure', *J Environ Manage*, vol. 70, no. 2, pp. 101–107, 2004, doi: https://doi.org/10.1016/j.jenvman.2003.11.001.

[64] B. K. Ahring, M. Sandberg, and I. Angelidaki, 'Volatile fatty acids as indicators of process imbalance in anaerobic digestors', *Appl Microbiol Biotechnol*, vol. 43, no. 3, pp. 559–565, 1995, doi: 10.1007/BF00218466.

[65] M. Zeppilli, A. Mattia, M. Villano, and M. Majone, 'Three-chamber Bioelectrochemical System for Biogas Upgrading and Nutrient Recovery', *Fuel Cells*, vol. 17, no. 5, pp. 593–600, Oct. 2017, doi: https://doi.org/10.1002/fuce.201700048.

[66] X. Jin, Y. Zhang, X. Li, N. Zhao, and I. Angelidaki, 'Microbial Electrolytic Capture, Separation and Regeneration of CO_2 for Biogas Upgrading', *Environ Sci Technol*, vol. 51, no. 16, pp. 9371–9378, Aug. 2017, doi: 10.1021/acs.est.7b01574.

[67] M. Zeppilli, M. Simoni, P. Paiano, and M. Majone, 'Two-side cathode microbial electrolysis cell for nutrients recovery and biogas upgrading', *Chemical Engineering Journal*, vol. 370, pp. 466–476, 2019, doi: https://doi.org/10.1016/j.cej.2019.03.119.

[68] A. Kokkoli, Y. Zhang, and I. Angelidaki, 'Microbial electrochemical separation of CO_2 for biogas upgrading', *Bioresour Technol*, vol. 247, pp. 380–386, 2018, doi: https://doi.org/10.1016/j.biortech.2017.09.097.

[69] M. Zeppilli, P. Paiano, C. Torres, and D. Pant, 'A critical evaluation of the pH split and associated effects in bioelectrochemical processes', *Chemical Engineering Journal*, vol. 422, p. 130155, 2021, doi: https://doi.org/10.1016/j.cej.2021.130155.

[70] J. Xiao, A. Kuc, T. Frauenheim, and T. Heine, 'CO_2 reduction at low overpotential on Cu electrodes in the presence of impurities at the subsurface', *J Mater Chem A Mater*, vol. 2, no. 14, pp. 4885–4889, 2014, doi: 10.1039/C3TA14755J.

[71] Y. Hori, K. Kikuchi, and S. Suzuki, 'Production of CO and CH_4 in electrochemical reduction of CO_2 at metal electrodes in aqueous hydrogencarbonate solution', *Chem Lett*, vol. 14, no. 11, pp. 1695–1698, Nov. 1985, doi: 10.1246/cl.1985.1695.

[72] K. P. Kuhl, E. R. Cave, D. N. Abram, and T. F. Jaramillo, 'New insights into the electrochemical reduction of carbon dioxide on metallic copper surfaces', *Energy Environ Sci*, vol. 5, no. 5, pp. 7050–7059, 2012, doi: 10.1039/C2EE21234J.

[73] Y. Hori, 'Electrochemical CO_2 Reduction on Metal Electrodes', in *Modern Aspects of Electrochemistry*, C. G. Vayenas, R. E. White, and M. E. Gamboa-Aldeco, Eds., New York, NY: Springer New York, 2008, pp. 89–189. doi: 10.1007/978-0-387-49489-0_3.

[74] F. Geppert, D. Liu, M. van Eerten-Jansen, E. Weidner, C. Buisman, and A. ter Heijne, 'Bioelectrochemical Power-to-Gas: State of the Art and Future Perspectives', *Trends Biotechnol*, vol. 34, no. 11, pp. 879–894, 2016, doi: https://doi.org/10.1016/j.tibtech.2016.08.010.

[75] C. Liu *et al.*, 'Enhancement of Bioelectrochemical CO_2 Reduction with a Carbon Brush Electrode via Direct Electron Transfer', *ACS Sustain Chem Eng*, vol. 8, no. 30, pp. 11368–11375, Aug. 2020, doi: 10.1021/acssuschemeng.0c03623.

[76] P. Batlle-Vilanova, S. Puig, R. Gonzalez-Olmos, A. Vilajeliu-Pons, M. D. Balaguer, and J. Colprim, 'Deciphering the electron transfer mechanisms for biogas upgrading to biomethane within a mixed culture biocathode', *RSC Adv*, vol. 5, no. 64, pp. 52243–52251, 2015, doi: 10.1039/C5RA09039C.

[77] Q. Yin *et al.*, 'Enhanced methane production in an anaerobic digestion and microbial electrolysis cell coupled system with co-cultivation of Geobacter and Methanosarcina', *Journal of Environmental Sciences*, vol. 42, pp. 210–214, 2016, doi: https://doi.org/10.1016/j.jes.2015.07.006.

[78] R. Blasco-Gómez, P. Batlle-Vilanova, M. Villano, M. D. Balaguer, J. Colprim, and S. Puig, 'On the Edge of Research and Technological Application: A Critical Review of Electromethanogenesis', *Int J Mol Sci*, vol. 18, no. 4, 2017, doi: 10.3390/ijms18040874.

[79] J. Park, B. Lee, D. Tian, and H. Jun, 'Bioelectrochemical enhancement of methane production from highly concentrated food waste in a combined anaerobic digester and microbial electrolysis cell', *Bioresour Technol*, vol. 247, pp. 226–233, 2018, doi: https://doi.org/10.1016/j.biortech.2017.09.021.

[80] M. Li *et al.*, 'Toward Excellence of Transition Metal-Based Catalysts for CO_2 Electrochemical Reduction: An Overview of Strategies and Rationales', *Small Methods*, vol. 4, no. 7, p. 2000033, Jul. 2020, doi: https://doi.org/10.1002/smtd.202000033.

[81] G. L. De Gregorio, T. Burdyny, A. Loiudice, P. Iyengar, W. A. Smith, and R. Buonsanti, 'Facet-Dependent Selectivity of Cu Catalysts in Electrochemical CO_2 Reduction at Commercially Viable Current Densities', *ACS Catal*, vol. 10, no. 9, pp. 4854–4862, May 2020, doi: 10.1021/acscatal.0c00297.

[82] Y. Hori, I. Takahashi, O. Koga, and N. Hoshi, 'Electrochemical reduction of carbon dioxide at various series of copper single crystal electrodes', *J Mol Catal A Chem*, vol. 199, no. 1, pp. 39–47, 2003, doi: https://doi.org/10.1016/S1381-1169(03)00016-5.

[83] H. Mistry, F. Behafarid, R. Reske, A. S. Varela, P. Strasser, and B. Roldan Cuenya, 'Tuning Catalytic Selectivity at the Mesoscale via Interparticle Interactions', *ACS Catal*, vol. 6, no. 2, pp. 1075–1080, Feb. 2016, doi: 10.1021/acscatal.5b02202.

[84] Z. Wang, G. Yang, Z. Zhang, M. Jin, and Y. Yin, 'Selectivity on Etching: Creation of High-Energy Facets on Copper Nanocrystals for CO_2 Electrochemical Reduction', *ACS Nano*, vol. 10, no. 4, pp. 4559–4564, Apr. 2016, doi: 10.1021/acsnano.6b00602.

[85] C. Tang *et al.*, 'CO_2 Reduction on Copper's Twin Boundary', *ACS Catal*, vol. 10, no. 3, pp. 2026–2032, Feb. 2020, doi: 10.1021/acscatal.9b03814.

[86] T. Cheng, Y. Huang, H. Xiao, and W. A. I. I. I. Goddard, 'Predicted Structures of the Active Sites Responsible for the Improved Reduction of Carbon Dioxide by Gold Nanoparticles', *J Phys Chem Lett*, vol. 8, no. 14, pp. 3317–3320, Jul. 2017, doi: 10.1021/acs.jpclett.7b01335.

[87] Y. Li, F. Cui, M. B. Ross, D. Kim, Y. Sun, and P. Yang, 'Structure-Sensitive CO_2 Electroreduction to Hydrocarbons on Ultrathin 5-fold Twinned Copper Nanowires', *Nano Lett*, vol. 17, no. 2, pp. 1312–1317, Feb. 2017, doi: 10.1021/acs.nanolett.6b05287.

[88] J. Monzó *et al.*, 'Enhanced electrocatalytic activity of Au@Cu core@shell nanoparticles towards CO_2 reduction', *J Mater Chem A Mater*, vol. 3, no. 47, pp. 23690–23698, 2015, doi: 10.1039/C5TA06804E.

[89] Z. Chang, S. Huo, W. Zhang, J. Fang, and H. Wang, 'The Tunable and Highly Selective Reduction Products on Ag@Cu Bimetallic Catalysts Toward CO_2 Electrochemical Reduction Reaction', *The Journal of Physical Chemistry C*, vol. 121, no. 21, pp. 11368–11379, Jun. 2017, doi: 10.1021/acs.jpcc.7b01586.

[90] C.-J. Chang *et al.*, 'Dynamic Reoxidation/Reduction-Driven Atomic Interdiffusion for Highly Selective CO_2 Reduction toward Methane', *J Am Chem Soc*, vol. 142, no. 28, pp. 12119–12132, Jul. 2020, doi: 10.1021/jacs.0c01859.

[91] X. Guo *et al.*, 'Composition dependent activity of Cu-Pt nanocrystals for electrochemical reduction of CO_2', *Chemical Communications*, vol. 51, no. 7, pp. 1345–1348, 2015, doi: 10.1039/C4CC08175G.

[92] J. Huang *et al.*, 'Potential-induced nanoclustering of metallic catalysts during electrochemical CO_2 reduction', *Nat Commun*, vol. 9, no. 1, p. 3117, 2018, doi: 10.1038/s41467-018-05544-3.

[93] J. Qiao, Y. Liu, F. Hong, and J. Zhang, 'A review of catalysts for the electroreduction of carbon dioxide to produce low-carbon fuels', *Chem Soc Rev*, vol. 43, no. 2, pp. 631–675, 2014, doi: 10.1039/C3CS60323G.

[94] M. Mikkelsen, M. Jørgensen, and F. C. Krebs, 'The teraton challenge. A review of fixation and transformation of carbon dioxide', *Energy Environ Sci*, vol. 3, no. 1, pp. 43–81, 2010, doi: 10.1039/B912904A.

[95] J.-P. Jones, G. K. S. Prakash, and G. A. Olah, 'Electrochemical CO_2 Reduction: Recent Advances and Current Trends', *Isr J Chem*, vol. 54, no. 10, pp. 1451–1466, Oct. 2014, doi: https://doi.org/10.1002/ijch.201400081.

[96] X. Lu, D. Y. C. Leung, H. Wang, M. K. H. Leung, and J. Xuan, 'Electrochemical Reduction of Carbon Dioxide to Formic Acid', *ChemElectroChem*, vol. 1, no. 5, pp. 836–849, May 2014, doi: https://doi.org/10.1002/celc.201300206.

[97] E. J. Dufek, T. E. Lister, and M. E. McIlwain, 'Influence of Electrolytes and Membranes on Cell Operation for Syn-Gas Production', *Electrochemical and Solid-State Letters*, vol. 15, no. 4, p. B48, 2012, doi: 10.1149/2.010204esl.

[98] X. Mao and T. A. Hatton, 'Recent Advances in Electrocatalytic Reduction of Carbon Dioxide Using Metal-Free Catalysts', *Ind Eng Chem Res*, vol. 54, no. 16, pp. 4033–4042, Apr. 2015, doi: 10.1021/ie504336h.

[99] M. Rammal, *Electrochemical Reduction of CO_2 to Low-Molecular-Weight Organic Molecules*. McGill University (Canada), 2016.

[100] H. Noda, S. Ikeda, Y. Oda, and K. Ito, 'Potential Dependencies of the Products on Electrochemical Reduction of Carbon Dioxide at a Copper Electrode', *Chem Lett*, vol. 18, no. 2, pp. 289–292, Feb. 1989, doi: 10.1246/cl.1989.289.

[101] J. J. Kim, D. P. Summers, and K. W. Frese, 'Reduction of CO_2 and CO to methane on Cu foil electrodes', *J Electroanal Chem Interfacial Electrochem*, vol. 245, no. 1, pp. 223–244, 1988, doi: https://doi.org/10.1016/0022-0728(88)80071-8.

[102] K. S. Lackner, 'Capture of carbon dioxide from ambient air', *Eur Phys J Spec Top*, vol. 176, no. 1, pp. 93–106, 2009, doi: 10.1140/epjst/e2009-01150-3.

[103] M. Gattrell, N. Gupta, and A. Co, 'Electrochemical reduction of CO_2 to hydrocarbons to store renewable electrical energy and upgrade biogas', *Energy Convers Manag*, vol. 48, no. 4, pp. 1255–1265, 2007, doi: https://doi.org/10.1016/j.enconman.2006.09.019.

[104] J. Z. Xia, M. Jodecke, A. P. S. Kamps, and G. Maurer, 'Solubility of CO_2 in (CH_3OH+H_2O)', *J Chem Eng Data*, vol. 49, no. 6, pp. 1756–1759, 2004.

[105] T. Mizuno, M. Kawamoto, S. Kaneco, and K. Ohta, 'Electrochemical reduction of carbon dioxide atTi and hydrogen-storing Ti electrodes inKOH–methanol', *Electrochim Acta*, vol. 43, no. 8, pp. 899–907, 1998, doi: https://doi.org/10.1016/S0013-4686(97)00252-1.

[106] L. L. Snuffin, L. W. Whaley, and L. Yu, 'Catalytic Electrochemical Reduction of CO_2 in Ionic Liquid $EMIMBF_3Cl$', *J Electrochem Soc*, vol. 158, no. 9, p. F155, 2011, doi: 10.1149/1.3606487.

[107] B. A. Rosen *et al.*, 'Ionic Liquid-Mediated Selective Conversion of CO_2 to CO at Low Overpotentials', *Science (1979)*, vol. 334, no. 6056, pp. 643–644, Nov. 2011, doi: 10.1126/science.1209786.

[108] B. Hu, C. Guild, and S. L. Suib, 'Thermal, electrochemical, and photochemical conversion of CO_2 to fuels and value-added products', *Journal of CO2 Utilization*, vol. 1, pp. 18–27, 2013, doi: https://doi.org/10.1016/j.jcou.2013.03.004.

[109] G. Centi and S. Perathoner, *Green carbon dioxide: advances in CO_2 utilization*. John Wiley & Sons Inc, 2014.

[110] B. Kumar, M. Llorente, J. Froehlich, T. Dang, A. Sathrum, and C. P. Kubiak, 'Photochemical and Photoelectrochemical Reduction of CO_2', *Annu Rev Phys Chem*, vol. 63, no. 1, pp. 541–569, Apr. 2012, doi: 10.1146/annurev-physchem-032511-143759.

[111] S. Zhang, P. Kang, and T. J. Meyer, 'Nanostructured Tin Catalysts for Selective Electrochemical Reduction of Carbon Dioxide to Formate', *J Am Chem Soc*, vol. 136, no. 5, pp. 1734–1737, Feb. 2014, doi: 10.1021/ja4113885.

[112] C. W. Li and M. W. Kanan, 'CO_2 Reduction at Low Overpotential on Cu Electrodes Resulting from the Reduction of Thick Cu_2O Films', *J. Am. Chem. Soc*, vol. 134, p. 46, 2012, doi: 10.1021/ja3010978.

[113] W. Paik, T. N. Andersen, and H. Eyring, 'Kinetic studies of the electrolytic reduction of carbon dioxide on the mercury electrode', *Electrochim Acta*, vol. 14, no. 12, pp. 1217–1232, 1969, doi: https://doi.org/10.1016/0013-4686(69)87019-2.

[114] Y. Hori and S. Suzuki, 'Electrolytic Reduction of Carbon Dioxide at Mercury Electrode in Aqueous Solution', *Bull Chem Soc Jpn*, vol. 55, no. 3, pp. 660–665, Mar. 1982, doi: 10.1246/bcsj.55.660.

[115] B. Deng, M. Huang, X. Zhao, S. Mou, and F. Dong, 'Interfacial Electrolyte Effects on Electrocatalytic CO_2 Reduction', *ACS Catal*, vol. 12, no. 1, pp. 331–362, Jan. 2022, doi: 10.1021/acscatal.1c03501.

[116] S. Kaneco, H. Katsumata, T. Suzuki, and K. Ohta, 'Electrochemical reduction of carbon dioxide to ethylene at a copper electrode in methanol using potassium hydroxide and rubidium hydroxide supporting electrolytes', *Electrochim Acta*, vol. 51, no. 16, pp. 3316–3321, 2006, doi: https://doi.org/10.1016/j.electacta.2005.09.025.

[117] A. Murata and Y. Hori, 'Product Selectivity Affected by Cationic Species in Electrochemical Reduction of CO_2 and CO at a Cu Electrode', *Bull Chem Soc Jpn*, vol. 64, no. 1, pp. 123–127, Jan. 1991, doi: 10.1246/bcsj.64.123.

[118] G. Z. Kyriacou and A. K. Anagnostopoulos, 'Influence CO_2 partial pressure and the supporting electrolyte cation on the product distribution in CO_2 electroreduction', *J Appl Electrochem*, vol. 23, no. 5, pp. 483–486, 1993, doi: 10.1007/BF00707626.

[119] S. Verma, X. Lu, S. Ma, R. I. Masel, and P. J. A. Kenis, 'The effect of electrolyte composition on the electroreduction of CO_2 to CO on Ag based gas diffusion electrodes', *Physical Chemistry Chemical Physics*, vol. 18, no. 10, pp. 7075–7084, 2016, doi: 10.1039/C5CP05665A.

[120] Y. Hori, A. Murata, and R. Takahashi, 'Formation of hydrocarbons in the electrochemical reduction of carbon dioxide at a copper electrode in aqueous solution', *Journal of the Chemical Society, Faraday Transactions 1: Physical Chemistry in Condensed Phases*, vol. 85, no. 8, pp. 2309–2326, 1989, doi: 10.1039/F19898502309.

[121] H. Zhong, K. Fujii, and Y. Nakano, 'Effect of $KHCO_3$ Concentration on Electrochemical Reduction of CO_2 on Copper Electrode', *J Electrochem Soc*, vol. 164, no. 9, p. F923, 2017, doi: 10.1149/2.0601709jes.

[122] N. Aryal *et al.*, 'Increased carbon dioxide reduction to acetate in a microbial electrosynthesis reactor with a reduced graphene oxide-coated copper foam composite cathode', *Bioelectrochemistry*, vol. 128, pp. 83–93, 2019, doi: https://doi.org/10.1016/j.bioelechem.2019.03.011.

[123] M. S. Sajna *et al.*, 'Electrochemical system design for CO_2 conversion: A comprehensive review', *J Environ Chem Eng*, vol. 11, no. 5, p. 110467, 2023, doi: https://doi.org/10.1016/j.jece.2023.110467.

[124] N. Hossain, M. A. Chowdhury, A. K. M. P. Iqbal, A. K. M. F. Ahmed, and M. S. Islam, 'Corrosion behavior of aluminum alloy in NaOH and Syzygium Samarangense solution for environmental sustainability', *Current Research in Green and Sustainable Chemistry*, vol. 5, p. 100254, 2022, doi: https://doi.org/10.1016/j.crgsc.2021.100254.

[125] A. F. Salvador *et al.*, 'Carbon nanotubes accelerate methane production in pure cultures of methanogens and in a syntrophic coculture', *Environ Microbiol*, vol. 19, no. 7, pp. 2727–2739, Jul. 2017, doi: https://doi.org/10.1111/1462-2920.13774.

[126] D. Örnek, A. Jayaraman, T. K. Wood, Z. Sun, C. H. Hsu, and F. Mansfeld, 'Pitting corrosion control using regenerative biofilms on aluminium 2024 in artificial seawater', *Corros Sci*, vol. 43, no. 11, pp. 2121–2133, 2001, doi: https://doi.org/10.1016/S0010-938X(01)00005-1.

[127] W. L. Bai, Y. Zhang, and J. N. Wang, 'Continuous Capture and Reduction of CO_2 in an Electrochemical Molten-Salt System with High Efficiency', *ACS Sustain Chem Eng*, vol. 11, no. 42, pp. 15364–15372, Oct. 2023, doi: 10.1021/acssuschemeng.3c04205.

[128] S. J. Pirt, D. W. Harty, I. Salmon, and Y.-K. Lee, 'Methanogenic digestion of glucose plus yeast extract by a defined bacterial consortium: Carbon balances and growth yields in chemostat culture', *Journal of Fermentation Technology*, vol. 65, no. 2, pp. 159–172, 1987, doi: https://doi.org/10.1016/0385-6380(87)90160-9.

[129] D.-M. Piao, Y.-C. Song, G.-G. Oh, D.-H. Kim, and B.-U. Bae, 'Contribution of Yeast Extract, Activated Carbon, and an Electrostatic Field to Interspecies Electron Transfer for the Bioelectrochemical Conversion of Coal to Methane', *Energies (Basel)*, vol. 12, no. 21, 2019, doi: 10.3390/en12214051.

[130] K. Kim, P. Wagner, K. Wagner, and A. J. Mozer, 'Catalytic Decomposition of an Organic Electrolyte to Methane by a Cu Complex-Derived In Situ CO_2 Reduction Catalyst', *ACS Omega*, vol. 8, no. 44, pp. 41792–41801, Nov. 2023, doi: 10.1021/acsomega.3c06440.

[131] D. Wakerley *et al.*, 'Bio-inspired hydrophobicity promotes CO_2 reduction on a Cu surface', *Nat Mater*, vol. 18, no. 11, pp. 1222–1227, 2019, doi: 10.1038/s41563-019-0445-x.

[132] W. Lu *et al.*, 'Microbial Electrochemical CO_2 Reduction and In-Situ Biogas Upgrading at Various pH Conditions', *Fermentation*, vol. 9, no. 5, 2023, doi: 10.3390/fermentation9050444.

[133] G. Kanellos, D. Kyriakopoulos, G. Lyberatos, and A. Tremouli, 'Electrochemical characterization of a microbial electrolysis cell during the bio-electrochemical conversion of CO_2 to CH_4', *Biochem Eng J*, vol. 182, p. 108431, 2022, doi: https://doi.org/10.1016/j.bej.2022.108431.

[134] Y. Huang *et al.*, 'Fabrication of Rambutan-like Activated Carbon Sphere/Carbon Nanotubes and Their Application as Supercapacitors', *Energy & Fuels*, vol. 35, no. 9, pp. 8313–8320, May 2021, doi: 10.1021/acs.energyfuels.1c00189.

[135] H. M. Alayan, M. A. Alsaadi, M. K. AlOmar, and M. A. Hashim, 'Growth and optimization of carbon nanotubes in powder activated carbon for an efficient removal of methylene blue from aqueous solution', *Environ Technol*, vol. 40, no. 18, pp. 2400–2415, Aug. 2019, doi: 10.1080/09593330.2018.1441911.

[136] Ch. M. Veziri *et al.*, 'Growth and optimization of carbon nanotubes in activated carbon by catalytic chemical vapor deposition', *Microporous and Mesoporous Materials*, vol. 110, no. 1, pp. 41–50, 2008, doi: https://doi.org/10.1016/j.micromeso.2007.09.002.

[137] S. Rathinavel, K. Priyadharshini, and D. Panda, 'A review on carbon nanotube: An overview of synthesis, properties, functionalization, characterization, and the application', *Materials Science and Engineering: B*, vol. 268, p. 115095, 2021, doi: https://doi.org/10.1016/j.mseb.2021.115095.

[138] L. M. Esteves, H. A. Oliveira, and F. B. Passos, 'Carbon nanotubes as catalyst support in chemical vapor deposition reaction: A review', *Journal of Industrial and Engineering Chemistry*, vol. 65, pp. 1–12, 2018, doi: https://doi.org/10.1016/j.jiec.2018.04.012.

Appendices

Appendix A: Thesis task description signed copy.

University of South-Eastern Norway

Faculty of Technology, Natural Sciences and Maritime Sciences, Campus Porsgrunn

FM4017 Project

Title: Electrochemical systems of CO_2 reduction on carbon nanotube electrodes for biogas production using microbes as catalyst

Supervisor: Nabin Aryal, Md. Salatul Islam Mozumder, Vafa Ahmadi, Raghunandan Ummethala, Britt Margrethe Emilie Moldestad

External partner:

Task background:

Microbial electrosynthesis (MES) is an emerging technology that utilizes carbon dioxide (CO_2) as feedstock for fuel and chemical production. In MES, electroactive microbes use the electron from the cathode and reduce CO_2. The double chamber 100 mL lab scale MES reactor consists of an anode and cathode separated by a membrane will be used to test. This thesis aims to investigate the electroreduction of CO_2 conversion into CH_4 on carbon nanotube-coated aluminium electrodes (Al/CNTs) with the assessment of current generation and methane production efficiency.

Objective: -
The primary aim of this project work is: -
1. To develop the CH_4 production process from CO_2 reduction.
2. To evaluate the effect carbon nanotube-coated aluminium electrodes (Al/CNTs) on CO_2 reduction rate.
3. MSc thesis writing and preparation for scientific article writing.

Student category: (EET or PT students)

Is the task suitable for online students (not present at the campus)? No

Practical arrangements:
The necessary accessories and instruments will be provided. The supervisor will provide the experiment set-up and operational training at USN.

Supervision:
As a general rule, the student is entitled to 15-20 hours of supervision. This includes the necessary time for the supervisor to prepare for supervision meetings (reading material to be discussed, etc.).

Signatures: Supervisor (date and signature): Nabin Aryal October 1st, 2023

Students (write clearly in all capitalized letters + date and signature): RAHUL BISWAS

October 1st, 2023

Appendix B: The thermodynamic potentials calculation of CO_2 reduction half reactions.

A fundamental calculation was used to determine the standard reduction potentials of an electrochemical process. The reduction and oxidation potential of water; $E^o_{H_2O|O_2} = 1.23$ V, and standard Gibbs free energy; $G_{CH_4} = -50.75$ kJ/mol, $G_{O_2} = 0$ kJ/mol, $G_{CO_2} = -394.36$ kJ/mol, and $G_{H_2O} = -394.36$ kJ/mol, must be known before calculating the reduction potential for CO_2.

I. Overall redox reaction:

$$CO_2 + 2H_2O \rightarrow CH_4 + 2O_2$$

II. Two half reaction:

Cathode half reaction: $CO_2 + 8H^+ + 8e^- \rightarrow CH_4 + 2H_2O$

Anode half reaction: $4H_2O \rightarrow 8H^+ + 8e^- + 2O_2$

III. Gibbs free energy of formation caltulation:

$$\Delta G = G_{products} - G_{reactants} = (G_{CH_4} + 2 \times G_{O_2}) - (G_{CO_2} + 2 \times G_{H_2O})$$

$$\Delta G = \{(-50.75) + 2 \times 0\} - \{(-394.36) + 2 \times (-237.1)\} = 817.81 \text{ kJ/mol}$$

IV. Cell potential calculation:

$$E^o_{cell} = -\frac{\Delta G}{nF} = -\frac{817.81 \times 1000}{8 \times 96485} = -1.06 \text{ V}$$

V. Cathode potential vs. SHE calculation:

$$E^o_{cell} = E^o_{CO_2|CH_4} - E^o_{H_2O|O_2}$$

$$E^o_{SHE\ (CO_2|CH_4)} = E^o_{cell} + E^o_{H_2O|O_2} = (-1.06) + 1.23 = 0.17 \text{ V}$$

VI. The use Nernst equation to correct at pH = 7:

$$E^{o}_{SHE\ at\ pH\ 7\ (CO_2|CH_4)} = E^{o}_{SHE\ (CO_2|CH_4)} - \frac{2.303 \times RT}{nF} \log\left(\frac{[reduction]}{[oxidation]}\right)$$

$$E^{o}_{SHE\ at\ pH\ 7\ (CO_2|CH_4)} = E^{o}_{SHE\ (CO_2|CH_4)} - \frac{2.303 \times RT}{nF} \log\left(\frac{[CH_4] \times [H_2O]^2}{[CO_2] \times [H^+]^8}\right)$$

$$E^{o}_{SHE\ at\ pH\ 7\ (CO_2|CH_4)} = E^{o}_{SHE\ (CO_2|CH_4)} - \frac{2.303 \times RT}{nF} \log\left([H^+]^{-8}\right)$$

$$E^{o}_{SHE\ at\ pH\ 7\ (CO_2|CH_4)} = E^{o}_{SHE\ (CO_2|CH_4)} - \frac{2.303 \times 8 \times RT}{nF} \times \{-\log([H^+])\}$$

$$E^{o}_{SHE\ at\ pH\ 7\ (CO_2|CH_4)} = E^{o}_{SHE\ (CO_2|CH_4)} - \frac{2.303 \times 8 \times RT}{nF} \times pH$$

$$E^{o}_{SHE\ at\ pH\ 7\ (CO_2|CH_4)} = 0.17 - \frac{2.303 \times 8 \times 8.314 \times 298}{8 \times 96485} \times 7 = -0.244\ V$$

VII. Cathode potential vs. Ag|AgCl calculation at pH = 7 using reduction potential shifts 0.0592 V per pH unit and 0.197 V potential difference between the SHE and Ag|AgCl scale:

$$E^{o}_{SHE\ (CO_2|CH_4)} = 0.197 + 0.0592 \times pH + E^{o}_{Ag|AgCl\ at\ pH\ 7\ (CO_2|CH_4)}$$

$$E^{o}_{Ag|AgCl\ at\ pH\ 7\ (CO_2|CH_4)} = E^{o}_{SHE\ (CO_2|CH_4)} - 0.197 - 0.0592 \times pH$$

$$E^{o}_{Ag|AgCl\ at\ pH\ 7\ (CO_2|CH_4)} = 0.17 - 0.197 - 0.0592 \times 7 = -0.441\ V$$

Appendix C: CH_4 production composition through electrochemical CO_2 reduction.

Table A.1 Amount of CH_4 production through CO_2 conversion.

Ex 2-Batch	Days	CH_4 (%)	CO_2 (%)	CH_4 (mL)	CO_2 (mL)
1	5	1.71	98.29	0.51	29.49
	10	4.08	95.92	1.22	28.78
	15	2.61	97.39	0.78	29.22
	20	22.84	77.16	6.85	23.15
2	4	5.75	94.25	1.72	28.28
	8	18.97	81.03	5.69	24.31
	11	0.00	100.00	0.00	30.00
	13	0.00	100.00	0.00	30.00
3	5	10.95	89.05	3.29	26.71
	10	10.40	89.60	3.12	26.88
	15	21.16	78.84	6.35	23.65
	20	20.01	79.99	6.00	24.00

Appendix D: Production efficiency parameter of electrochemical reaction experiment.

Table A.2 CH_4 production efficiency parameter of electrochemical experiment.

Parameter	**Ex 2-Batch 1**	**Ex 2-Batch 2**	**Ex 2-Batch 3**
CO_2 conversion efficiency (%)	8.47	14.10	18.53
Faradic efficiency (%)	9.67	31.26	18.39
Energy efficiency (%)	1.64	5.30	3.12
Current density (mA/cm^2)	-0.346	-0.062	-0.488
Charge (C)	-3057.5	-748.2	-3217.7

Appendix E: Chemical composition analysis during electrochemical CO_2 reduction.

Table A.3 pH, alkalinity, total-COD, and soluble-COD content during electrochemical reaction.

Ex 2-Batch	Days	pH	Alkalinity (mg/L)	Total-COD (mg/L)	Soluble-COD (mg/L)
1	0	7.00	2530	2530	250
	5	8.34	-	-	-
	10	7.80	-	-	-
	15	7.60	6430	2650	1715
	20	7.90	3460	6430	250
2	0	7.00	5544	1790	1395
	4	7.50	7340	5170	985
	8	7.41	1550	5770	1120
	11	7.44	5110	8780	1410
	13	7.22	7404	2080	1035
3	0	7.00	1870	1295	835
	5	8.00	3358	1010	1275
	10	7.91	4264	1185	595
	15	8.13	7132	1595	550
	20	7.86	7888	1270	565

Appendix F: VFAs analysis during electrochemical CO_2 reduction.

Table A.4 VFAs concentration during electrochemical CO_2 reduction.

Ex 2-Batch	Days	Acetic acid (mg/L)	Propionic acid (mg/L)	Isobutyric acid (mg/L)	Butyric acid (mg/L)	Isovaleric acid (mg/L)	n-valeric acid (mg/L)	Isocaproic acid (mg/L)	Heptanoic acid (mg/L)
1	0	2.38	0.18	0.41	-	2.10	-	-	-
	15	-	-	-	13.52	0.95	0.72	-	-
	20	19.75	10.24	-	3.37	3.82	-	-	-
2	0	6.42	0.64	-	-	1.95	-	-	-
	4	4.41	1.97	2.61	1.73	2.06	-	1.09	0.40
	8	1.94	0.89	0.64	0.60	0.98	-	0.55	-
	11	15.31	1.73	-	-	0.80	-	0.60	-
	13	1.83	0.61	-	-	0.82	-	0.25	-
3	0	1.14	1.12	-	-	0.06	-	0.19	-
	5	0.74	0.23	0.54	0.23	0.46	-	-	-
	10	0.21	0.06	0.11	0.05	0.15	-	-	-
	15	1.12	0.13	0.10	0.07	0.16	-	-	-
	20	0.56	0.13	-	0.09	0.06	-	-	-